Non-Invasive Acoustic Emission Testing of Compressed Trabecular Bone and Porous Ceramics using Seismic Analysis Techniques

A Thesis
Presented to
The Academic Faculty

By

Gaylon C. Hollis

Georgia Institute of Technology
August 30, 2004

Non-Invasive Acoustic Emission Testing of Compressed Trabecular Bone and Porous Ceramics using Seismic Analysis Techniques

Approved by:

Dr. Kenneth Cunefare, Advisor

Dr. Robert Guldberg, Advisor

Dr. Christopher Lynch

Date Approved: 8/30/2004

TABLE OF CONTENTS

LIST OF TABLES

LIST OF FIGURES

LIST OF ABBREVIATIONS

Acoustic Emission	AE
Decibel	dB
Gutenberg Richter	GR
Hit definition Time	HDT
Hit Lockout Time	HLT
Mechanical Testing System	MTS
Microcomputer Tomography	MicroCT
Peak Definition Time	PDT

SUMMARY

Acoustic emission(AE) is one of the most sensitive techniques to non-invasively monitor deformation, fatigue, and fracture of many materials. The purpose of this study was to evaluate the potential to use AE to detect local failure events within porous ceramic materials. The primary material of interest was mineralized trabecular bone. A better understanding of the failure of trabecular bone is highly relevant to skeletal fragility diseases such as osteoporosis.

This study sought to develop a post processing technique that could strengthen the relation between the events detected and the phenomena occurring as a specimen is loaded. The deficiency in other techniques is that they did not fully make a quantitative correlation between acoustic emission event characteristics and the physical occurrence of damage events. The study evaluated the use of seismic power laws because these laws were able to attach a quantitative model to an earthquake and its successive aftershocks. Earthquake transmission has similar propagation attributes when compared to acoustic emission; seismic waves radiate from the epicenter of an earthquake. Acoustic waves radiate from the source of energy release in an acoustic emission event.

The study measured the acoustic emission response of trabecular bone and highly oriented ceramics. The bone and ceramics were extracted in two perpendicular directions so that the structural orientation was different. The study sought to evaluate if the power-laws could differentiate the acoustic emission response based on varying the material and varying the structural orientation. The samples were quasi-statically compressed; the mechanical and acoustic emission data were simultaneously recorded.

The study found that using the seismic power-law did not statistically differentiate the directional orientation for trabecular bone or ceramic specimens. Acoustic emission did indicate that event detection was different for each type of material. Correlations were established with the acoustic emission response and the mechanical testing data. These relationships were explainable because of the mechanical properties of the material.

CHAPTER 1: INTRODUCTION

1.1 Motivation

Osteoporosis is a disease that attacks the structural integrity of trabecular bone. The disease weakens the structure of the bone by increasing porosity and decreasing bone remodeling. Trabecular bone is important because its primary biomechanical function is to absorb energy and distribute joint loads. The heterogeneous chemical composition and variable structural orientation increases the complexity of evaluating the fracture and yield characteristics. Current techniques, such as ultrasound and x-ray, evaluate the porosity of bone. Their main disadvantage is that they introduce energy into the specimen in the form of acoustic pulses and radiation; both have been shown to be harmful to biological tissue. (Miller 2004)

The other techniques introduce energy through a transmitter and the resulting response at the receiver determines how the energy is altered. Acoustic emission differs from the other techniques because it only receives a response when an event occurs. The study at hand used acoustic emission as a monitoring technique in compressing bovine trabecular bone specimens**.** The overall intent was to develop an acoustic emission monitoring technique that can discriminate material parameters based on the acoustic response to mechanical loading .

1.2 Purpose

The reason for the study was to lay additional groundwork in using acoustic emission as a technique for evaluating the damage and fracture properties in trabecular bone. The study evaluated seismic power laws as a post-processing method in order to statistically differentiate material and direction strut orientation from the acoustic emission data of quasi-statically compressed specimens. For acoustic emission (AE) to achieve its full potential as a technique that aids in the understanding of material failure mechanisms, the generated signals must be quantitatively related to physical attributes, such as dislocation motion, slip, stress, or stress intensity factor. A sound post-processing model for acoustic emission data was anticipated to improve the correlation between acoustic emission events and fracture characteristics.

Power-law models were developed by seismologist to categorize earthquakes. (Reasenberg 1989) These relationships were used because force-induced acoustic emission propagates through an experimental specimen in the same way that seismic waves propagate through the earth. The seismic quantities that are calculated using the relationships provide a link to plate-slipping in earthquakes. The study sought to provide the same form of quantification for trabecular bone instead of the semi-quantitative correlations that are currently in place. (Konstankiewicz 2000)

1.3 Specific Aims

The first specific aim was to determine if the power-laws could differentiate bone and ceramics by the acoustic emission response.

Hypothesis 1: The parameters of the power-laws will be statistically different when comparing the acoustic emission response for bone and ceramic.

The second specific aim was to determine if the power-laws could differentiate structural orientation when comparing the acoustic emission response.

Hypothesis 2: The parameters of the power-laws will be statistically different when comparing the acoustic emission response for horizontally and vertically oriented specimens of the same material.

The third specific aim was to determine if acoustic emission could monitor micro-damage in addition to micro-fracture. Micro-damage was anticipated to occur in loading the sample before the sample's yield point.

Hypothesis 3: There will be a noticeable acoustic emission response for bone specimens loaded in the elastic region.

1.4 Description of Acoustic Emission

Acoustic emission (AE) is one of the most sensitive techniques to non-invasively monitor deformation, fatigue, and fracture of many materials. Acoustic emission is acoustic waves generated by the release of energy from localized sources in a material subjected to an externally applied stimulus.(Kohn 1995) When deformation causes damage, multiple forms of energy are released. AE focuses on the portion that is released as acoustic wave energy. Transducers attached to a specimen convert acoustic impulses to a voltage; data acquisition software adjusts the voltage to an event magnitude in decibels(dB). Figure 1 is a depiction of an acoustic emission event. The anatomy of an event is characterized by the peak amplitude, event duration, rise time, energy and

counts. The peak amplitude is the maximum magnitude for an event. Counts are the instances where the event exceeds the threshold. The duration is the time period between the first count and the last count. The rise time is the period between the initial event detection and the peak amplitude.

In viewing Figure 1, it is important to note that a threshold magnitude must be set. The threshold voltage is selected to differentiate between electronic noise and an actual event. For example, Figure1 shows that two events occurred; within each event 5 and 4 counts occurred respectively. The figure also shows that an event suddenly rises to a peak value and then decays below the threshold; this is referred to as the ring down.

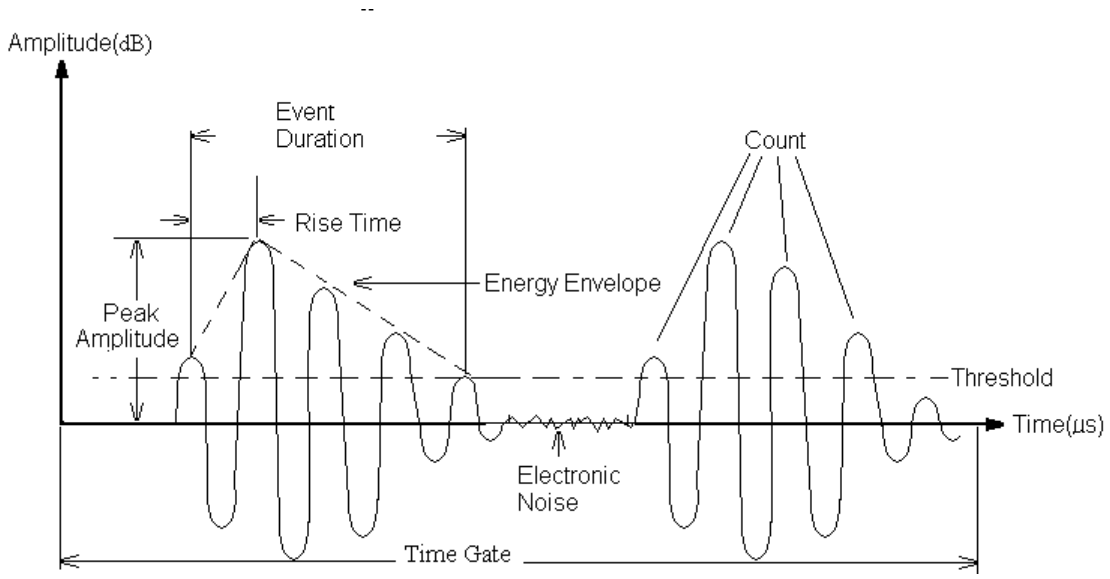

Figure 1: Schematic View of Acoustic Emission Event

1.5 Factors influencing acoustic emission

Any factor that affects the propagation of an acoustic wave through a material will influence the characteristics of the resultant AE signal.(Kohn 1995) The material

factors include: crystal structure, texture (porosity), orientation, anisotropy, grain size, morphology, material history, thermal history, strength, and purity. For example, the mechanical factor of mechanical history refers to any previous stress or loading mode placed on the specimen. Previously applied stress must be exceeded before any further AE can be detected; this phenomenon is referred to as the Kaiser Effect. Thus in testing, it is beneficial in a compressive test of trabecular bone to perform each test with a different sample to eliminate mechanical history as a source of error. Figure 2 is a depiction of the Kaiser Effect. In the post yield region, the trabecular bone is compacted to a material with the same chemical composition but different structure. The figure shows that compaction in the post-yield region will induce additional acoustic emission after the initial maximum stress is exceed.

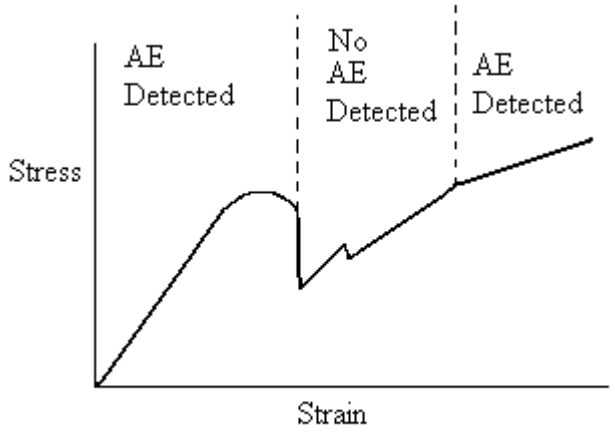

Figure 2. Schematic of Kaiser effect.

The experiments did not seek to answer the dependence of the numerous material factors. The scope of the experiments treated the material factor interdependencies as a black box. The primary material factor evaluated was the material orientation.

The experimental factors are not inherent in a material; they can be altered for an experiment. The experimental factors are strain rate, test temperature and testing direction. Due to the numerous combinations of mechanical and experimental factors, it should be noted that the relationship between AE signals and material failure mechanisms is therefore complex with numerous interdependent parameters influencing AE sources.

1.6 Advantages and Disadvantages of Acoustic Emission

The principal difference between AE and the conventional techniques of ultrasound or dual x-ray photon absorptometry (DEXA) is that no energy is introduced into the system. DEXA introduces harmful radiation. The energy deposited by ultrasound can cause cavitations within tissues.(Miller 2004) In comparison to these damage detecting techniques, AE has certain advantages.

The first advantage is that AE tests run continually. An x-ray only produces a before-measurement and after-measurement, but tells nothing about what happens in between exposures. The second advantage is that AE can detect damage at multiple sites and sites of unknown spatial coordinates. The spatial arrangement of transducers can be adjusted to triangulate the origin of an event. The damage site can be determined by using attenuation characteristics and array dimensions to calculate position based on the time a transducer in the array receives an event. The most important advantage is that AE is non destructive, which means it has future applications for clinical diagnosis. The events are transmitted and the transducers detect a response.

AE's initial disadvantage is that it is not easily calibrated so repetitive tests cannot be repeated and compared in different environments. For example, the same calibrations for the transducers and settings with the software will not always yield the same results

for two experimenters. The second disadvantage is that there is no physical connection between acoustic emission data and the structural damage. AE needs to answer the question, how does the properties of the events or the number of events quantitatively relate to the micro-damage and micro-fracture of trabecular struts?

The study sought to involve a technique that could strengthen the relationship between the acoustic events detected and the phenomena occurring as a specimen is loaded. Background and previous research indicated that earlier studies did not fully quantify the physical connection to acoustic emission events. The current study used seismic power laws because these power laws were able to attach a quantitative model to an earthquake and its successive aftershocks.

1.7 Power law analysis

The power-law analysis of acoustic emission began with developing a relationship between acoustic emissions and seismic propagation through the principle of self-similarity. The principle of self-similarity is the appearance of identical features at different scales. The term fractal is used to describe self-similar objects; by definition a fractal set is scalar invariant. The relationship that correlates a fractal set is a power-law relationship. The fractal connection exhibited by seismic power laws relates a fracture distribution to magnitude. Overall, scalar invariance can be applied to bone because the wave propagation properties through rock and bone are both induced by a sudden release of energy. Because of the similar wave propagation phenomena, a correlation between fracture distribution and acoustic emission amplitude can be established.(Hatton 1993)

The seismic models used were the Gutenberg-Richter relationship (G-R) and Omori's Law. The following sections will lay out the background of the two power laws and their use in the analysis of acoustic emission. The discussion will involve evaluating the two laws over two time domains. The first domain is the cumulative domain; it consists of the initial loading to the failure of the sample, which ranges from 1 to 3 minutes. The second time domain is the discrete domain; it is the duration of a single acoustic emission event, which ranges from 10 to 25 microseconds. Due to the mathematical properties of the power laws, the G-R relationship and Omori's law provide a fit for the acoustic response. Omori's law is more representative of the ring down effect in a single event. The G-R relationship can be used to put quantitative parameters towards the cumulative distribution of events' amplitudes over the entire test.

1.7.1 Gutenberg-Richter Relationship

The first model is the Gutenberg-Richter relationship. The Gutenberg-Richter relationship characterizes the cumulative amplitude distribution as a power law function where

$$Log\ N(W) = a - b|W|. \quad (1)$$

The form of the equation suggests that data can be modeled linearly. $N(W)$ is the number of earthquake events of a size greater than or equal to the magnitude (W). In the case of acoustic emission, W is the amplitude of each event measured in decibels (dB) for each event. The a-value is a constant and b is the seismic b-value.(Aue 1998) Figure 3 is an example of the graphical method used to evaluate the values in the equation. A linear regression is performed on the distribution; the a-value and b-value are calculated based

on the linear regression equation of the distribution of the magnitude and their occurrences. The *b*-value, which is a slope, represents the rate of hit acquisition, so the *b*-value is correlated to fracture rate over the duration of the test. The value of -0.053 in the regression equation is the *b*-value. The magnitude of the *b*-value is compared between groups since all *b*-values will be negative.

The *a*-value is the intersection of the maximum magnitude with the y-axis: it is calculated by solving the regression equation at *x* equals the maximum amplitude. In this figure, *x* equals 64 dB, so the *a*-value is .3. Unlike the *b*-value, the interpretation of the *a*-value is not based on the absolute value, so an *a*-value of -0.5 is "less productive" than 0.3. The physical significance of the *a*-value is that it is the productivity of the event; it relates an event's propensity to create aftershocks. A high *a*-value means that an initial shock produced many aftershocks. A low *a*-value means that aftershock output was small for the size of the main shock. Thus, the *a*-value is a function of the maximum amplitude over the entire test.(Reasenberg 1989)

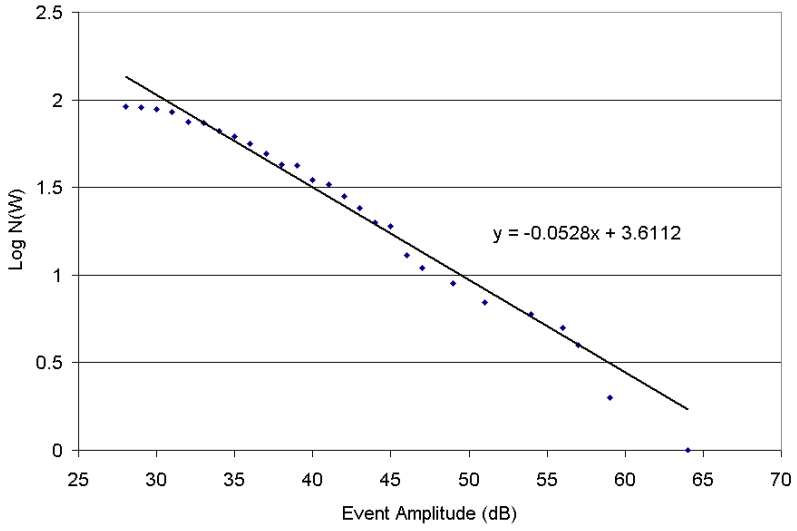

Figure 3: Example of Gutenberg Richter relationship calculations for a sample

1.7.2 Omori's law

The second model is Omori's law. Omori's law is an exponential power law function, which states

$$N(t)=t^{-m} \quad (2)$$

N(t) refers to the number of counts above the threshold within a single event. The *m*-value indicates the exponential rate of count occurrence. The *m*-value is calculated by performing a power-equation regression using numerical analysis to match the time distribution of the counts within a single event. Figure4 shows how the difference in decay rates affects the distribution. The graph indicates that an increase in the *m*-value leads to a steeper graph. A high *m*-value is characteristic of short burst events.

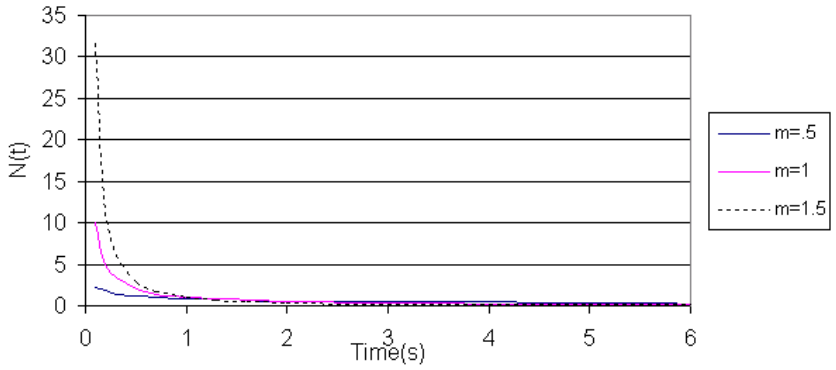

Figure 4:Effect of *m*-value change on decay rate

Figure 5 depicts an example of the power-law regression used determine the *m*-value for a set of data within an event. The value of 1.6733 is the rate of decay and is used as the *m*-value

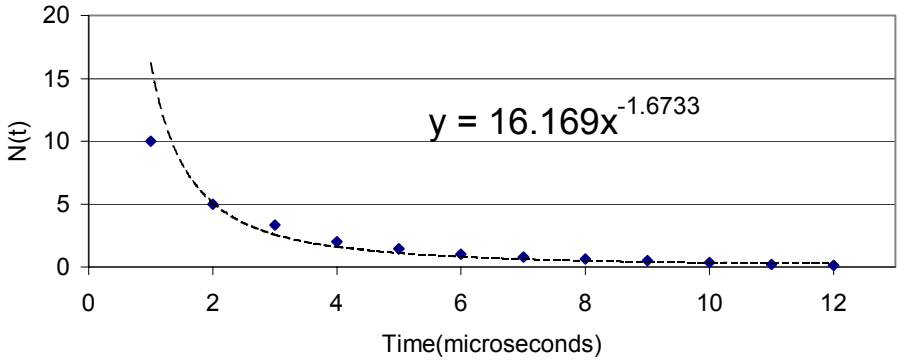

Figure 5:Power law regression for the time distribution of counts with in an event

Omori's law is anticipated to be more useful in single hit analysis; it is applicable to an individual event analysis because the exponential function will produce a model with a limit of zero as time (*t*) approaches infinity. The decaying function resembles the ring down shown by an event in Figure1. Upon further inspection of Omori's Law, *N(t)* is a function of time. Therefore, the time at which each aftershock(count) occurs must be known to calculate the *m*-value. In order to use Omori's Law in acoustic emission data analysis, software must be able to provide the time stamp of each count with in an event. A specimen under compressive loading may yield a range of 50 to 2000 events in a minute. Within each event, a time stamp must be placed on each of the counts within an event, which lasts 10 to 30 microseconds. The software must capture, process and store excessive amounts of data in nanoseconds.

Once the hardware and software are configured to capture the time data for each count's data, Omori's law must be rescaled. In earthquake analysis, the *t*-value of Omori's Law is based on days. However, the *t*-value needs to be rescaled and reevaluated based on the duration of acoustic emission events. During experimental design, a determination must be made in regards to the *t*-value used. The *t*-value should

either be a standardized value or the duration of each hit. Using a standardized *t*-value allows the comparison of *m*-values for a respective magnitude to be compared across each experimental group because a baseline window time has been set. The disadvantage of a standardized time window is that for events longer than the standard *t*-value is that counts will be omitted from processing. The second option of a *t*-value is the actual duration of the hit, which would give more information about what is actually happening in a hit. However, it would be harder to make comparisons across groups. For example, events of the same magnitude will not always yield the same number of counts due to the material's structural variability. In the study at hand, Omori's law was not implemented because it was initially inferred that the software would not record the proper data. Further analysis into the data file structure indicated that an algorithm could be devised. Further study in this area would seek build an effective algorithm to apply Omori's Law to each event.

1.7.3 Predictive Capabilities of power law model

The use of the two power-law models has another property. The seismic power-laws are used to predict phenomena in addition to characterizing the phenomena. It is possible to combine the two in such a way that one can find the rate of counts of magnitude **W** or greater at time *t* after a main shock of magnitude $\mathbf{W}_m$. In order to combine the formulas, the Gutenberg-Richter relation is converted to a non-logarithmic form, to match the Omori's law.

$$log\ N(W) = a - b\ (\ W - W_m) \quad (3)$$

and raise each side to the power of 10, so that the left-hand side is no longer *log N(W),* but simply *N(W)*:

$$N(W) = 10^{a - b(W-W_m)} \quad (4)$$

Now that the G-R equation is in this form, the two independent equations are combined into one function with two variables:

$$Rate(t, W) = 10^{a - b(W-W_m)} * (t)^{-m} \quad (5)$$

It is possible to convert this equation to solve for the probability that one or more aftershocks(counts) in a given magnitude range will occur within a specified time range. The probability *P*, of one or more earthquakes occurring in the magnitude range (*W1<W<W2*) and the time range (*T1<t<T2*) is

$$P = 1 - \exp[-\int_{W1}^{W2}\int_{T1}^{T2} Rate(t,W)dtdW] \quad (6)$$

This allows seismologists to make probability forecasts for aftershock sequence activity. For example, at one week after a magnitude 7 main shock, one would conclude that "there is a 40% chance of a magnitude 3 or larger aftershock in the next 15 days". (Reasenberg 1989)

When the combined model is applied to the trabecular bone, it has clinical implications. If a device is able to yield information about the temporal data within an event(i.e. the specific time the amplitude of a count occurs within an event), then the count patterns within an event can be predicted. Further analysis would seek to determine a relationship between the count pattern and physical phenomena. Overall, the assumption for Omori's law is conjecture for acoustic emission data analysis because no previous testing substantiates it.

1.8 Trabecular Bone Information

Trabecular bone is a complex structure because of its varying structure and heterogeneous composition. Bone tissue consists of cells embedded in a fibrous organic matrix of Type 1 collagen. The stiffness of bone is derived from the presence of mineral salts that permeate the organic matrix. The mineral comprises 75% of the weight and 50% of the volume; the minerals are calcium phosphate and calcium carbonate. (Hayes 1997)

Whole bones are composed of two types of bony tissue. Cortical bone comprises the diaphysis(shaft) of long bone and the thin shell that surrounds the epiphysis(ends). Trabecular bone is the second form of bone and is the focus of this study. Trabecular bone composes the interior of the epiphysis region of bone. Figure 6 shows the digital image of a right human femur; the regions that comprise the bone have been depicted. A directional cube has also been placed on the figure to indicate the direction of extraction with respect to biological terminology.

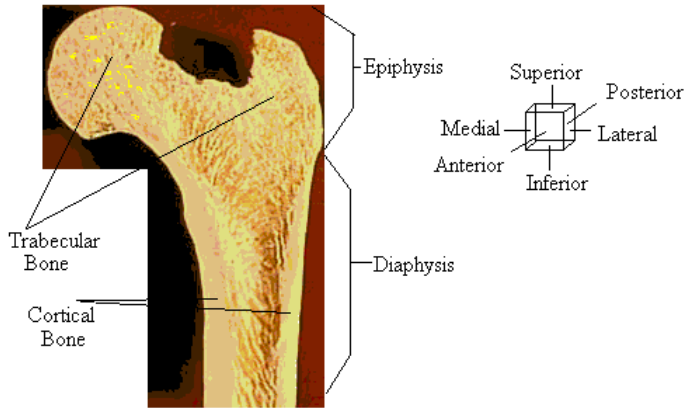

Figure 6: Digital Image of the proximal region of a right human femur with a directional cube of anatomical terminology

The structure of trabecular bone is comprised of plates and struts of varying composition. The porosity of trabecular bone ranges from 30 to 95%. The biomechanical feature of trabecular bone serves as an energy absorber and load distributor. As osteoporosis damages the trabecular struts, shock absorption decreases and brittle fractures increases. (Hayes 1997)

The direction of trabecular strut orientation is related to the direction in which the imposed stresses reach maximum and minimum values. The trabecular struts and plates tend to align and thicken in the directions that will support the load. The trabecular struts in bovine femurs are primarily oriented along the length of the shaft due to the fact that the principal loading is along the longitudinal shaft of the bone.

1.9 Power-law Studies and Acoustic Emission

The Gutenberg Richter relationship was used by Aue to characterize porous ceramics. The study found that the *b*-value(fracture rate) was inversely correlated to the fracture strength of the material. Therefore, the samples with higher strength were assumed to have a lower fracture rate. The stronger materials do not exhibit as much damage propagation(crack growth) was the weaker specimens. Thus failure occurs at higher amplitudes because higher loads are place on the specimen. An increase in the number of higher amplitude events lowers the slope(b-value) of the magnitude distribution. In addition to the power-law analysis, the study found that friction from the fracture planes sliding over each other caused AE events. (Aue 1998) The study assumed that the events were friction induced because the samples did not fail. These friction events exhibited low amplitudes and low number of counts, which were not characteristic

of the high amplitude events associated with specimen failure. Trabecular bone does not fracture like ceramic because it is a viscoelastic material. There is no current ability to distinguish a friction event from yielding event. The friction induced events were anticipated to occur as the trabecular struts slide past each other during compaction.

The seismic power-law analysis was used to evaluate brittles material such as rock and porous ceramic(Aue 1998). Trabecular bone was anticipated to have different acoustic emission properties than ceramics because it is a viscoelastic material. The events in the pre and post yield region are anticipated to be different because various damage-inducing phenomena are occurring.

The viscoelastic property implies that the material properties are time-dependent. Fischer conducted a study in which he found that the acoustic emission response is strain rate dependent. The tests were conducted at a high strain rate(.01mm/s) and low strain rate(.001mm/s). A greater number of events occurred at slower strain rates. However, the specimens tested at a greater strain rate had higher amplitude emissions. This correlation was explained by inference that the higher strain rate caused the bone to act more like a brittle material.(Fischer 1986) The events in brittle fractures are characterized by high amplitude and short duration events. The testing direction of the tests was in tension; events were not detected until the specimen was well into the plastic region. This suggests that there are multiple phenomena occurring when the testing direction is in compression, since events occur in the elastic and plastic region.

1.10 Mechanical Testing of Trabecular Bone

In relating AE to trabecular bone, bone acts in the same way as heterogeneous porous materials. Bone fails in distinct stages: initiation, stable crack growth and unstable crack propagation. Two important studies were completed in regards to bone's defects and bone's orientation. The first study showed that damaged trabecular bone exhibited a reduction in Young's Modulus and strength. The study also found that modulus reduced more than strength. The results were interpreted that trabecular bone was stress protected due to a redistribution of stress to undamaged bone.(Keaveny 1994) In the second study, damage was induced by loading the specimen into its plastic region. The results found that the modulus and strength were dependent on orientation of the trabecular struts.(Ford 1996) The affect of these studies imply that there are different acoustic emission properties due to the differences in orientation and structural integrity.(Morgan 2001)

Previous studies investigated acoustic emission and its relationship to characterizing properties of bone. Testing conducted by Hasegawa noted that in osteopenic human trabecular bone, micro-damage occurs at lower stress levels but has less events than normal bone once the plastic zone is reached. (Hasegawa 1993) The study allowed the researchers to infer that a normal bone will fail all at once due to a massive amount of micro-damage occurring once a maximum load is reached. The fact that less AE was generated in the more brittle deproteinized bone appears to be a

contradiction with the premise that brittle materials produce more hits. The stress however is not evenly distributed in trabecular bone because of the decreased density from osteoporosis. However, another interpretation might be that collagen damage is a source of AE in the post yield region; there is more collagen in the healthier bone. The AE data might also demonstrate that when bone yields, the resultant micro-structural damage enables further deformation without significant increases in load. Once this deformation occurs, further loading causes crack propagation and catastrophic fracture. The specimens used in the testing were notched in order produce a stress concentration. Damage induced in bone, through mechanical or chemical means leads to the generation of more AE and AE at lower levels of mechanical stimuli.(Kohn 1995)

In more clinical testing, researchers are using acoustic emission to understand the interfaces between bone and metal. The impact of the study shows that acoustic emission can detect differences in material because of changes in events. Due to the wear and tear that occurs at the hip, a replacement must be done every 10 years. Failure of the fixation in the femoral component of a total hip arhtroplasty is linked to the debonding of the bone cement and metal. Acoustic emission is used to monitor the fatigue; over the life of the fatigue cycle damage detected by AE can validate the reliability and integrity of a joint.(Davies 1996) During testing, a debonded surface will immediately become apparent. The researchers used ultrasound once failure was initiated to determine the mode of failure. Care had to be taken with ultrasound such that a false positive is not given for a debonded surface.(Davies 1996) Since the false positive can be achieved with ultrasound, it has disadvantages in being used in a compressive test.

1.11 Signifigance

The purpose of this study is to use power law models to establish a discernable difference in trabecular bone and ceramic specimens based on the orientation. The power law development is based on acoustic emissions during trabecular bone loading to seismic waves during an earthquake. The drive to make a correlation between acoustic emission and seismic analysis is supported because the physical relationship has been established for seismic studies.(Petri 1994)

After all preliminary research was completed, an experimental methodology was developed to carry out the specific aims. The next chapter discusses the hardware and software considerations that determine the scope and type of experiments that could be run.

CHAPTER 2. EXPERIMENTAL METHODOLOGY

This chapter contains hardware theory and software configurations that must be considered. The methodology entails the factors used in creating the experimental matrix for the test. The experimental matrix defines how the experiments are organized and executed. The hardware and software factors include the sensors, placement of the sensors on the specimen, digital signal filtering processes, and calibration techniques.

2.1 Theory of an Acoustic Emission signal and Calibration of Sensors

When an event occurs within the specimen, it propagates to the transducer. The external pressure on the transducer cause the a piezo-electric crystal in the transducer to resonate, converting a acoustic pulse into an electrical signal.(Davies 1996) Figure 7 is a schematic of a transducer manufactured by Dynasen. The figure's dimensions indicate the size of the transducer. The size and sensitivity was important when considering the appropriate transducer.

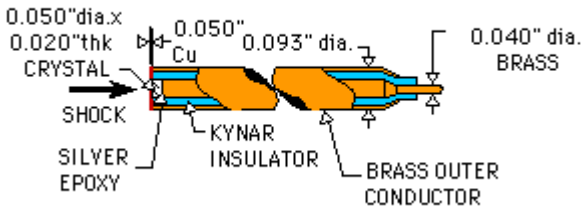

Figure 7: Dynasen acoustic emission transducer Model No. CA-1135

The transducer types differ in the resonant frequencies and sensitivities that they are expected to operate. When choosing a transducer, the sensitivity is dependent on the

resonant frequency and range of frequency. The resonant frequency for a transducer occurs at the highest decibel magnitude for known induced pressure.

2.2 Configuring software settings

In reviewing Figure1, the AE software must have the ability to differentiate between an entire event and the counts with in an event. Three settings in the data acquisition must be properly defined: The peak definition Time(PDT), Hit definition Time(HDT), and Hit Lockout Time(HLT). The PDT is the time of the true peak(maximum amplitude) of the AE waveform. To avoid a false measurement, the PDT should be set to be as short as possible, but longer than the anticipated rise time of the events. As show in Figure 8, setting the PDT larger than the rise time will insure the maximum decibel level is captured for an event.

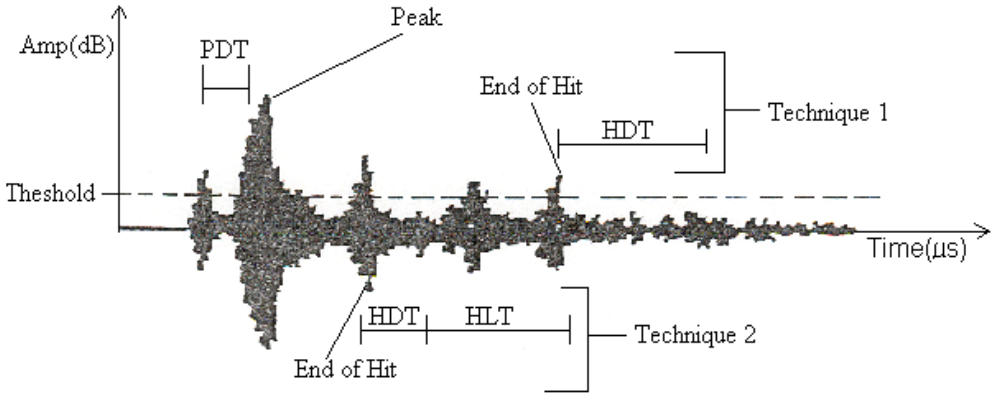

Figure 8:Depiction of filtering techniques for Acoustic Emission software

The most important setting is the HDT; it enables the system to determine the end of a hit. If the time is not properly defined, two short burst events could be lumped and characterized as a single event. There are two methods in determining the HDT for a

respective set of tests. The first technique is to make the HDT at least twice as large as the PDT. The principle behind the first technique is to include all consequences in the hit, such as reflections. The filter will include all reflections as part of the event until the time between peaks exceeds the HDT. The second technique of setting the HDT shortens the HDT from Technique 1 in order to disregard the reflections. The benefit of Technique 2 is that the event can clear the processing buffers quicker and be ready for the next event. The use of Technique 2 for the HDT has benefits when revisiting the issue of Omori's law applications in post processing individual events. The second technique is better suited to fit in the acoustic emission software to increase the efficiency and speed to which events are processed. Figure 8 shows a depiction of the difference between Technique 1 and 2 in defining the HDT.

The last setting is the Hit Lockout Time(HLT); it will inhibit the measurement of reflection and late arriving parts of an AE signal. A properly defined HLT will insure that each event within a set time-window corresponds to one event. The HLT only has an impact when used in conjunction with Technique 2 of the HDT. Figure 8 shows a depiction of a properly defined HLT. It was important to note that HLT's shorter that 300 microseconds were not meaningful since the software takes this time to complete measurements and transfer data.(Acoustics 1995)

2.3 Transducer Placement and Source location

After all of the software settings have been established, the proper usage and orientation of the transducers was researched. The geometry of the transducer array, difference in arrival times of the different transducers, and the wave velocities must be verified to locate the source of an event. The geometry of the transducer array involves

the spatial placement of each transducer on the specimen. Determining n-th dimensional plane of the source requires n+1 transducers. For example, locating a planar coordinate of a source would require a minimum of three transducers.(Qi 2000)

The difference in arrival times refers to a time in which an event reaches each transducer in the array. For example, an event should register a different time for each of the transducers unless in the unlikely case that the event is located geometrically in the center of the n-transducer array and the attenuation due to changes in material composition and structure have no affect on the propagating signal. Determination of the HDT is important setting when using AE if damage location is important. The last detail is verification of wave velocity; verification is initially completed to validate if the event detected is an actual event or electronic noise. Verification of wave velocity is an inherent portion of determining the difference in arrival times. The speed a signal reaches a transducer can be determined by the distance the transducer is from the source. Figure 9 is a schematic of the transducer array. Each of the transducers have a different location in respect to the source.

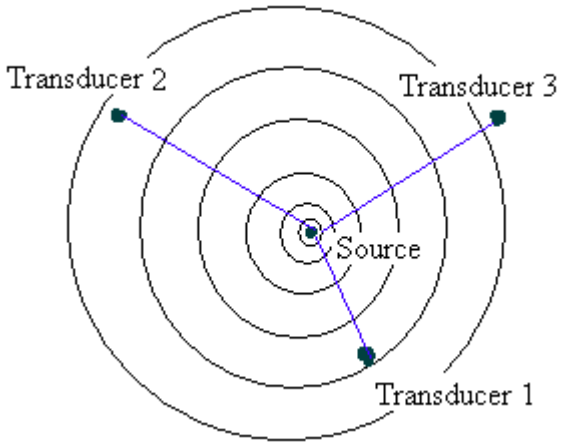

Figure 9:Transducer array used to determine a planar(2-D) coordinate

2.4 Attenuation Characteristics

In characterizing the acoustic emission events, their output relies on their velocity and attenuation. The events' propagation direction is assumed to be radially directed from the source. The attenuation of the signal is the measure of the loss of energy as the wave propagates through the material. The inherent properties of the material has the greatest impact on the attenuation properties. Attenuation is frequency dependent; the form of fracture mode such as shearing or compaction has different frequency content. For materials that are homogeneous and uniformly structured, an attenuation factor has been established. However, trabecular bone is highly heterogeneous and variably structured. Alves found that the correlation of bone mineral density to velocity and attenuation remain unaffected by the removal of marrow and replacement with water. The test did show that the removal of marrow decreased attenuation and increased velocity.(Alves 1996) The findings were useful in understanding signal propagation through marrow. The researched study is different from the study at hand because it was an ultrasonic test. An ultrasonic test has an emitter and receiver on two sides of the material. The speed at which the receiver captures the signal determines the attenuation that decreased the signal speed and strength. In the case of acoustic emission, the signal is generated within the sample, the initial speed and strength of the signal is not known. Therefore, the calculation of attenuation characteristics of acoustic emission events is complicated.

The effect of attenuation needs to be considered if AE is to proceed into established clinical use. For example, a respective transfer function has to be deduced to

account for the thickness and layers of soft tissues between the transducers and the fracture events. Frequency-dependent attenuation is the primary source of variations of the velocity of sound through bone.(Wear 2000) Therefore, the energy lost as the signal travels through bone, marrow, and tissue has a greater effect than scattering caused as the waves travel through the various mediums. Also, the orientation of the trabecular struts yielded significantly different values of attenuation coefficients.(Wear 2001)

2.5 Post-processing methods and time-scale considerations of analyzing data

The next step in developing an acoustic emission experiment was to evaluate the methods in which acoustic emission data was processed. It is important to understand that there is a difference in the quantitative and semi-qualitative correlations that exist when analyzing acoustic emission event. Currently, AE parameters are used to create a semi-quantitative correlation. The data does not lead to fully quantitative results because the information has yet to provide a direct link between the physical phenomena and the AE signal. For example, the quantitative connection between the voltage induced on the load cell and the force on the specimen is fully established. The semi-quantitative trends inferred from the AE data are matched with the experimental factors such as stress, strain rate and testing direction

The most common form of analyzing data is by summing the parameters over the duration of the entire test. For example, the sum of events can be related as a function of strain.(Konstankiewicz 2000) Figure10 is an example of the total cumulative event occurrence in relation to increasing strain.

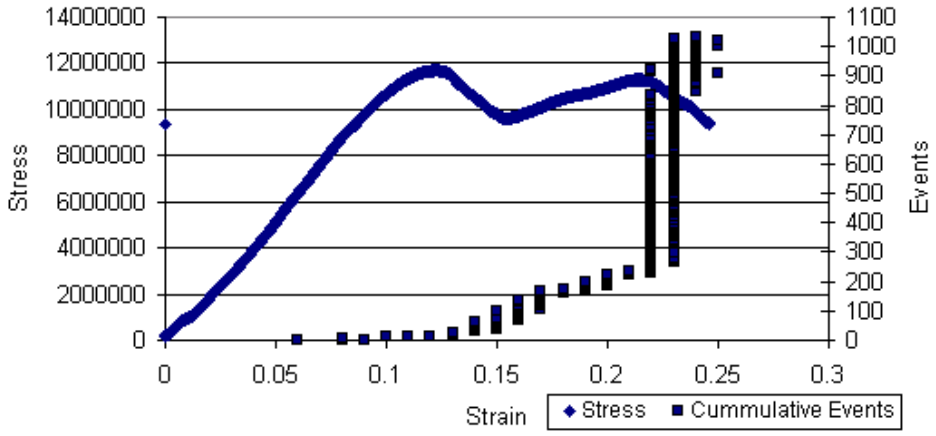

Figure 10: Stress and cumulative events vs. strain

Since AE is a time dependent data acquisition, it can be categorized into two time domains. The first domain is the cumulative domain and the second is the discrete time domain. The cumulative domain is the period of the entire test(initial loading to failure). The cumulative analysis would answer the question, "how many detectable events exceed the threshold over the entire period of the test?" The cumulative number of events would be related to strain rate, yield point or fracture point. For example, the question of " is there a significant change in the number of events as the specimen is compressed to yielding and fracture?" is answered in evaluating the cumulative domain. Besides the event itself , the only parameter within the event used is the amplitude of the event.

Dissecting the anatomy of a single event is more descriptive in analyzing the results of an event. Discrete domain analysis looks at trends of an individual event: more of the event data parameters, such as the counts, rise time, duration, energy and amplitude, are involved. A single event analysis is more informative in determining "how" the event was induced. For example, a high amplitude, short duration and low count is associated with a burst type emission. The sudden energy release is characterized

by the fracture of trabecular struts. Low amplitude, low count and long duration are assumed to be events occurring as the bone specimens are yielding.(Fischer 1986)

The hardware and software factors were evaluated to build an experiment that would evaluate the specific aims. The test matrix developed from the methodology is established in the next chapter. The most important factor was the analysis of the cumulative and discrete time scales' impact on the acoustic emission data.

CHAPTER 3: EXPERIMENTAL SETUP AND TESTING

The following chapters included the physical application of the methodology described in Chapter 2. The test rig was constructed to link the mechanical testing systems and acoustic emission data acquisition. The specimens were extracted from bovine tissue and ceramic blocks. Before the final experiments were conducted, the transducers were calibrated to detect emissions from the bone.

3.1 Experiment Hardware Setup

The experimental setup was comprised of two major systems. The first system in the experimental setup is the acoustic emission data acquisition hardware. The AE hardware consists of an AEDSP-32/16 board that was installed into a pc. The board processes data with a parallel digital signal processor (Texas Instruments TMS320C40). The board has two digital data acquisition channels, the transducers (Physical Acoustics S9225) used in the tests were connected to the channels. The board also has two input connections to receive parametric information from another system. The parametric information is the load and displacement output from the mechanical testing system.

The second system in the test apparatus is a digital servo-controlled electro-mechanical device(Test Resources 650R). A schematic of the test apparatus is shown in Figure11. The setup was devised to capture the real-time force and displacement for each event within the acoustic emission data file. The arrows in the figure show the direction of the data flow. All of the information is compiled in the acoustic emission data file.

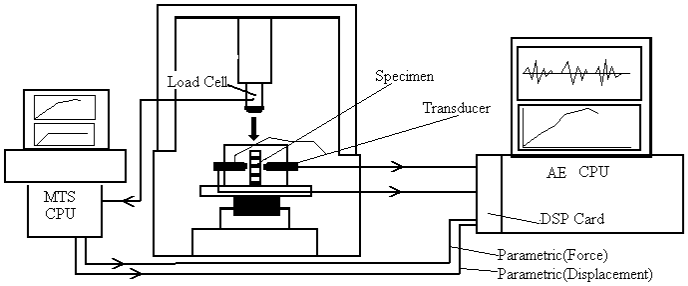

Figure 11: Schematic of test apparatus with direction of data acquisition

Figure 12 shows a magnification of the specimen holding rig. Increasing the normal force between the specimen and the transducer was important. During quasi-static compressive loading, the specimen may shift or bulge causing the transducer to slip off the specimen. The use of springs increased the normal force. The rig was also designed to provide easy transition between sample testing. After the specimen was unloaded, the pins were pulled away from the specimen. This further compressed the springs and removed normal force holding the specimen erect.

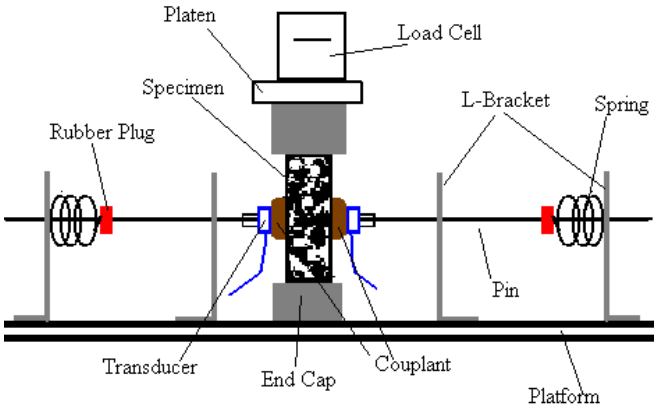

Figure 12: Specimen holder rig for compressive testing of specimens

3.2 Specimen Extraction

The specimens used in the test are trabecular bone specimens from the femurs of cows and Corning Celcor ceramic. The distal portion of the femur was used; it is the portion that connects the femur to the knee. The distal portion of the knee has a large surface area, which allowed more specimens to be extracted. A custom trephine was designed to extract the samples. The extracted specimens used are 6 mm in diameter and 18-20 mm in length. Each specimen's ends were leveled and placed in an end cap with a depth of 4mm. The end caps reduced the specimens testing length to 8-10 mm. A protocol was developed to prepare the samples for extraction and is detailed in Appendix B.

Biological directional terminology, such as superior/inferior and medial/lateral, is more exact than using vertical and horizontal. However, in order to draw similarity between the orientation of the ceramic and the bone the phrasing of vertical and horizontal orientation is used. As discussed earlier, the trabecular specimens are anticipated to orient along the direction of principal loading. Figure13 is a microcomputer tomography (micro-CT) image of trabecular bone extracted from the vertical (superior-inferior) with a microscopic view of vertically oriented sliced trabecular bone prepared through histology; Figure 14 is the same depiction but for horizontally oriented trabecular bone. The views depict that there is a difference in thickness for the specimens oriented in the vertical direction.

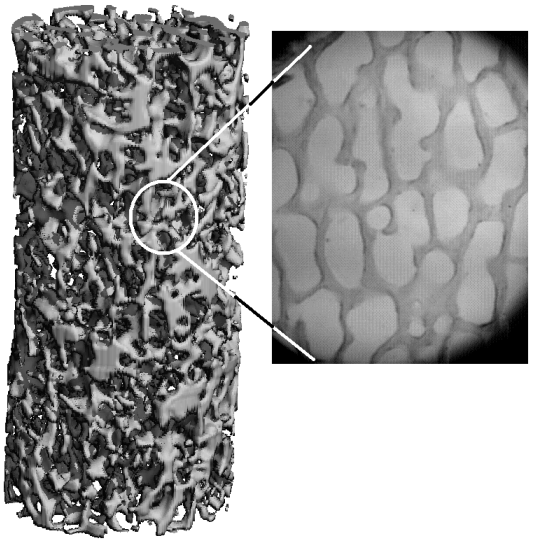

Figure 13: Micro -CT image and microscopic view of vertically oriented trabecular bone

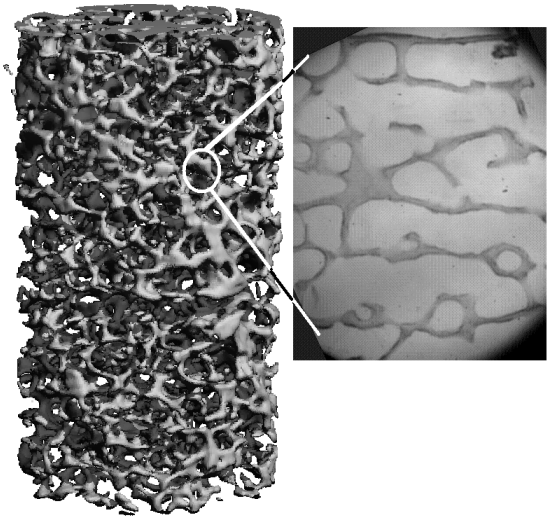

Figure 14: Micro-CT image and microscopic view of horizontally oriented trabecular bone

The ceramic specimens were extracted using the same size trephine to get samples of comparable size to the bone specimens. Figure 15 is a microcomputer tomography image of the ceramic cut in both the vertical and horizontal direction. The protocol is slightly different for the trabecular bone because biological waste considerations were not

important. Once the ceramic samples were extracted, the specimens were embedded in Crisco shortening. In order to embed the samples, the ceramic specimens were placed in the beaker of liquefied Crisco and allowed to cool. Crisco shortening was used to make the ceramic and trabecular bone specimens more similar. The shortening has the consistency most similar to the marrow in trabecular bone.

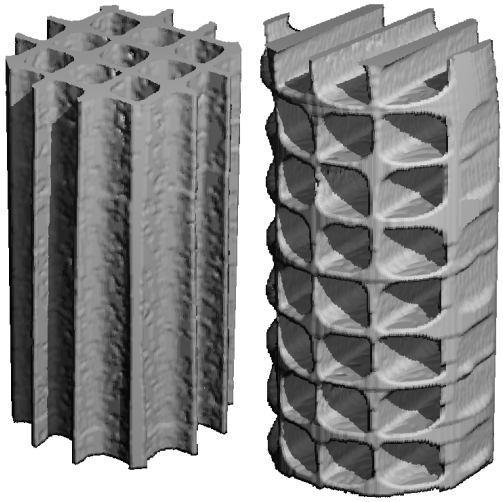

Figure 15: Vertically and horizontally oriented ceramic

The ceramics are used in the study because their structural orientation does not vary as much as the trabecular bone. The specimens also limited the variability of other material factors such as porosity and anisotropy. In addition, model values derived from the ceramic specimens can be compared to previous studies.

3.3 Test setup calibration.

Acoustic emission experiments are difficult to replicate because of the baseline values are dependent upon the sensitivity of the transducer, software and hard ware. The simplest form to test whether the experimental setup is properly recording events is to use

the pencil lead test. Loose pieces of pencil lead are broken in close proximity to the transducer. This has no bearing on the range of the data. The magnitude of a pencil lead break produces a burst event because it is a single break. (Wolfgang 1991)

The software package that operates the hard ware of the acoustic emission test system is the MISTRAS/MITRA program. In the program, proper calibrations and settings for the transducers must be set to record the proper signals. The settings are used to optimize signal reception involved in making adjustments to hardware and software.

Special care was taken to verify whether a signal is internal noise from the system or an actual hit. The preamplifier has three gain settings: 20dB, 40dB and 60dB. The settings on the preamplifier was optimized with the threshold level in the software to find the lowest threshold with discernable events. The hardware adjustment was initiated by varying the preamplifier setting. The value of the threshold was varied between 25 and 50(dB)

The calibration tests were qualitative in nature. Each setting was run twice to observe a trend. These tests were run to see if a signal was detected and how strong the response was. The tests were run in displacement control at a rate of .01mm/s and to a final value of 2 mm of compression. The 2 mm of compression was set to insure that the sample failed, since the assurance of events was desired. Each test was run on a different sample because compressing a sample twice would affect the compressive strength of the second test due to compaction, as earlier explained to the Kaiser effect.

3.3.1 Calibration Discussion

The analysis of the results was based on three factors, the presence electronic noise, the amplitude of events and the number of hits during the test. The worst results were found at a 20 dB gain on the preamplifier. The 60 dB gain on the pre-amplifier increased the sensitivity of the transducers, so electronic noise was significantly increased. The scope of the calibration was to optimize the sensitivity with the threshold level. In order to use the 60 dB gain, experiments would have to be to run on a higher threshold. This situation would have eliminated the hits that would have registered under threshold needed to eliminate the electronic noise.

The testing indicated that the 40 dB gain was the best setting for the preamplifier. Using the 40 dB gain is consistent with the preamplifier value used in other experiments.(Qi 2000) Once the preamplifier value was selected, the lowest threshold of 25 dB was used to insure that no hits were being missed. A threshold below 25 dB resulted in electronic noise.

3.4 Compressive Testing

The mechanical tests quasi-statically loaded the samples in uniaxial compression to failure at 0.01 mm/s. The high strain rate was used because higher amplitude events were desired. The load-deformation curve during mechanical testing was recorded and subsequently matched temporally to generation of AE signals from the sample.

The first experiment conducted was a quasi-static compressive loading of Corning ceramic(Celcor©). Once the specimens were prepared using the extraction protocol, the specimens were embedded in aluminum end-caps. The embedded

specimens were placed in the test rig of Figures 11 and 12. The specimens were loaded at .01mm/s to a final displacement of 2.5 mm. The acoustic emission events and stress strain information were simultaneously recorded. After the two ceramic groups were tested, the two trabecular bone groups were run through the same compressive testing.

3.5 Post Processing Procedures

The post-processing analysis involved turning the acoustic emission data in to the cumulative distribution of the amplitude magnitudes as shown in Figure2. At first, the acoustic emission data is converted to a text file using the MITRAS-ATASC file converter program. Table 1 shows an example of a partial file after it has been converted to a text file. Parametric 1 is the force data output from the mechanical testing system; Parametric2 is the displacement measurement from the MTS. The channel is the number of the respective transducer.

Table 1: Visual Representation of Converted Acoustic Emission File

Time	Parametric 1	Parametric 2	Channel	Rise time	Duration	Energy	Counts	Amplitude
6.055	0.25	0.09	1	1	1	0	7	25
6.373	0.26	0.09	1	1	1	0	3	25
6.406	0.26	0.09	2	2	1	0	2	25
6.565	0.26	0.09	2	1	1	0	6	30
6.638	0.26	0.09	1	1	1	0	2	27

A 0.2% strain calculation was performed on all of the tests to determine the yield point using the stress/strain plots from the MTS. Next, the time of the yield point for each sample was determined from the mechanical loading data and matched to the acoustic emission text file. Each file was run through a Matlab program to determine the logarithmic occurrence of each event's amplitude. The Matlab program is listed and commented in Appendix C.

3.6 Histology Testing

A qualitative histology study was done to address the third specific aim. The florescent image of micro-damage was compared to the acoustic emission response. The samples were loaded to 2% strain; chemical fluorescent marking was conducted before and after the specimen was tested. The specimens were then set in a polymerizing clear resin. The specimens were sliced to a thickness of 150 to 200 microns and placed on a slide. The thickness of 150 to 200 microns was used because it is the approximate thickness of a trabecular strut. The thickness allows the view of the microscope to focus on a single layer. The histology protocol is detailed in Appendix D

CHAPTER 4: RESULTS AND DISCUSSION

The results section contains the analysis of each of the three sets of tests. The first set comprised the loading of the vertically and horizontally oriented ceramic; the second set was the vertically and horizontally oriented bone. The third test was the histology study that was used to evaluate the visual damage that occurs in the elastic region. The discussion of the three tests is organized based on the specific aims introduced in Chapter1.

For first and second specific aim, the Gutenberg-Richter parameters, the maximum amplitude, average amplitude and cumulative events were compared using a 2-sample student t-test with a 95% confidence interval. The statistical test leads to a p-value. A p-value less than .05 indicated a statistical difference; a p-value greater than .05 and less than .10 indicated a statistical trend. A p-value higher than .10 indicated no statistical difference. The summary of the statistical results for the groups is contained in the Appendix A.

In the discussion, the quantitative relationships from the Gutenberg-Richter relationships will be analyzed. The statistical results were compared to the stress-strain information and other material factors that may have contributed to the results. Next, the semi-quantitative relationships, cumulative events maximum amplitude and average amplitude, were used to develop correlations between the acoustic emission data and mechanical data. Although the maximum amplitude is a semi-quantitative evaluation, it will serve as a transition between the GR relationship quantities and the other

relationships because the maximum amplitude affects the calculation of the *a*-value. As the maximum amplitude increases, the a-value becomes more negative.

The histology study addressed the third specific aim. The analysis compared the stress-strain information; the acoustic emission patterns detected while the sampled were mechanically tested; and the visual interpretation of the damage detected using the fluorescent microscope.

The purpose of the study was to evaluate the acoustic emission data. However, it was necessary to initially present the results of the mechanical testing because the mechanical data is a physical indication of how the materials were responding to loading. The Young's Modulus and yield strength of the material groups were calculated. Table 2 shows the Young's Modulus and strength for the bone and ceramic specimens. The yield times for the bone and fracture time for the ceramics are also included in the table.

Table 2: Mean Young's Modulus, strength and yield/fracture time for specimens

	yield time/ fracture time(sec.)	Strength(Mpa)	Modulus(Mpa)
vertical bone	145.9	9.0	66.3
horizontal bone	12.1	3.75	41.3
vertical ceramic	237.3	12.6	84.2
horizontal ceramic	83.3	5.36	81.3

The table indicates that the vertical ceramic is the strongest material; the horizontal bone was the weakest material. In both material cases, the vertically oriented group was more resilient to loading. Figure 16 and 17 is a graphical depiction of the modulus and strength for the groups, and the bars indicate the standard error. The only comparison that did not exhibit a statistical difference was the modulus comparison between the

vertical ceramic and horizontal ceramic. The reason for the similarity was inferred to be caused by the homogenous chemical composition of the ceramics.

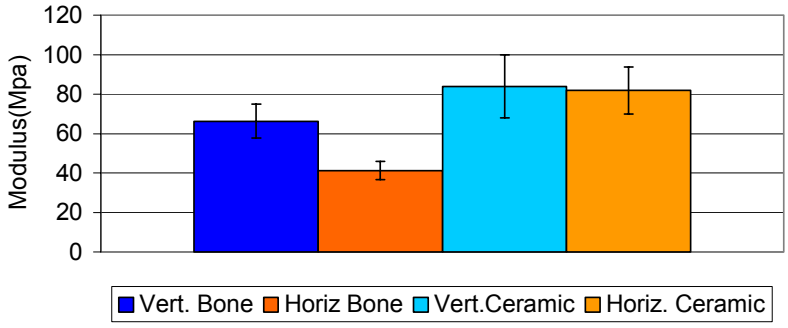

Figure 16:Mean Young's Modulus for all material groups

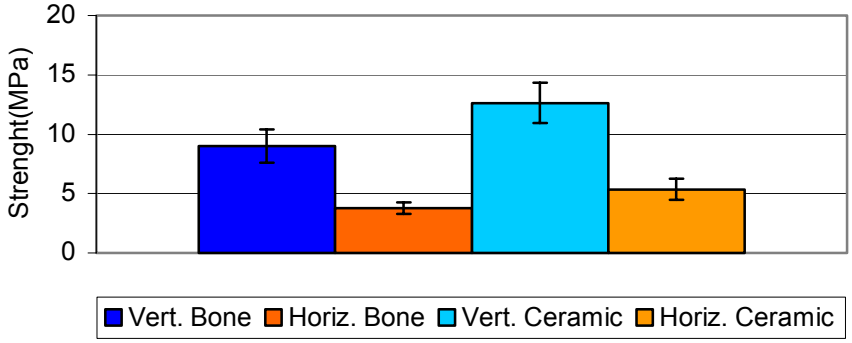

Figure17: Mean Strength for all material groups

4.1.1 Specific Aim 1(Vertical)

4.1.1.a Gutenberg Richter (Quantitative)

The first specific aim was to investigate the effect of material difference. The hypothesis for the first aim asserted that the Gutenberg-Richter parameters would be statistically different between material. The analysis evaluated the groups comprised of the same structural orientation and different material.

Figure18 shows the mean *b*-values of vertically oriented specimens. The vertical bone had a higher *b*-value than the vertical ceramic, and the vertical bone's strength was less than the vertical ceramic. A lower strength inducing a higher *b*-value is consistent with the results of a previous study and discussion in Chapter 1. (Aue 1998) The *b*-value was not found to be statistically different for the two groups(p=.81).

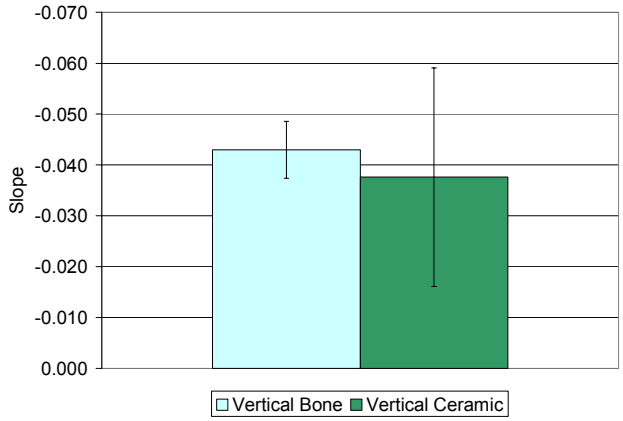

Figure 18: Fracture Rate(*b*-Value) for vertically oriented groups

Figure 19 displays the mean a-values for the two vertical groups. As a recapitulation, the a-value in seismicity is the productivity. As productivity increases, more aftershocks should be induced with the event. The *a*-value is calculated by using the linear regression equation at the highest magnitude recorded. Since the calculation of the *a*-value account for the sign, the negative and positive values lower the mean through cancellation. For the vertical ceramic the standard error is .26, which is higher than the mean. The situation with the vertical ceramic indicated a difference that occurs when attempting to adapt the seismic law to an analogous acoustic emission law. The combination of variability for the *b*-value and maximum amplitude is responsible for the skewed productivity results.

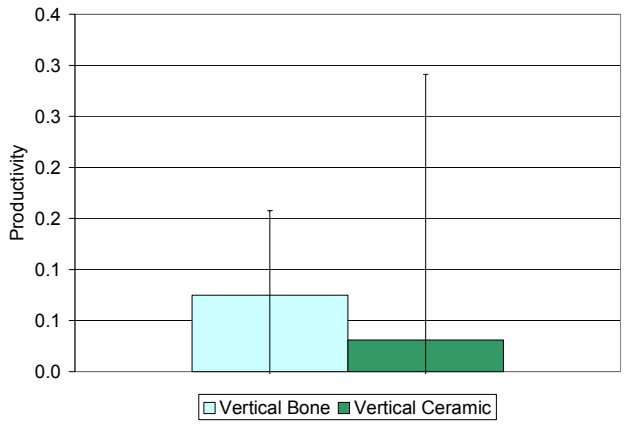

Figure 19 Productivity(*a*-value) for vertically oriented groups

4.1.1.b Maximum Amplitude, Average Amplitude, Cumulative Events (Semi-quantitative)

Figure 20 shows the mean maximum magnitudes for the vertical groups. The values were significantly different(p=.04). The maximum amplitude was anticipated to be directly correlated to the load placed on the specimen, which is shown in Table 2. This is because higher loads lead to higher amounts of energy release when damage occurs. The higher maximum amplitude for the vertically oriented ceramic is consistent with higher stress to induce failure.

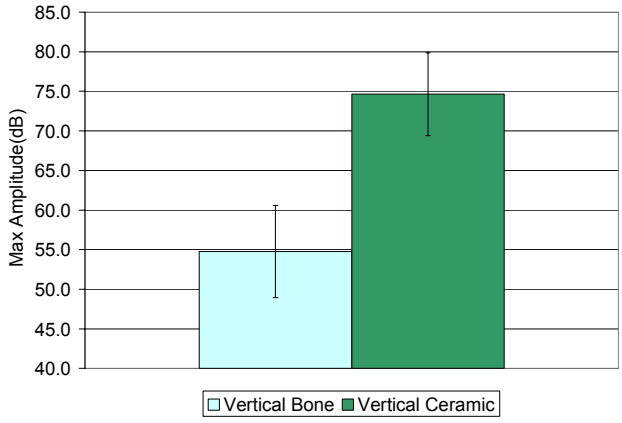

Figure20:Maximum amplitude of vertically oriented groups

Figure 21 shows that the average amplitude for the vertical bone is higher than the average amplitude of the vertical ceramic. A reason for the result was not initially clear. An inference to explain the reason was deduced when the average amplitude was compared between the horizontal groups.

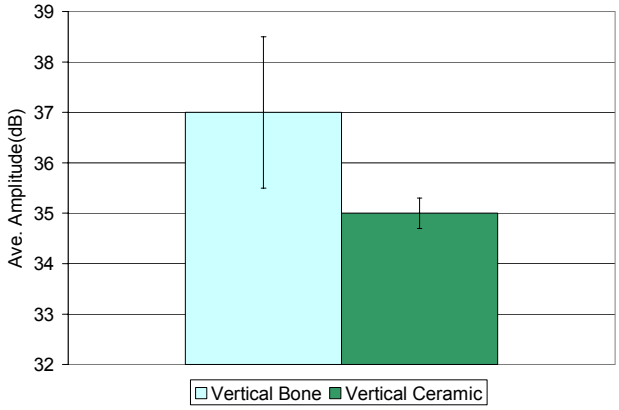

Figure 21 Average amplitude for vertically oriented groups

The strongest difference between vertical ceramic and bone was shown by the difference in cumulative events(p=.006). Figure 22 shows the mean value for the cumulative events. The vertical bone had 15 events and the vertical ceramic had over 3200.

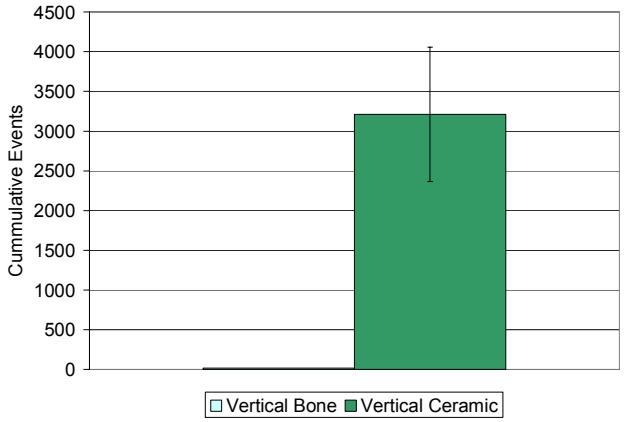

Figure 22 Cumulative events for the vertically oriented groups

The great disparity is because of the material differences. The ceramics do not yield like the viscoelastic bone specimens. The time consideration was a factor that affected the difference in cumulative events. Table 2 shows that vertical specimens took longer to fail than the vertical specimens took to yield. However, it is asserted that the failure mechanisms which affect ceramic specimens(i.e. slip, friction, fracture) induce more events than the vertical bone specimens or these fracture mechanisms are louder for the ceramics.

4.1.2 Specific Aim 1(Horizontal)

4.1.2.a Gutenberg Richter (Quantitative)

After the vertical groups were compared, the horizontal groups were analyzed. The *b*-value was found to be statistically different(p=.002). In explaining the occurrence, the data did not follow the trend that the specimen with the lower strength should have the higher *b*-value. The result show in Figure 23 is the first instance that the GR-relationship could be used to show a difference in material. The results do show that the trend of the weaker specimen have a lower fracture rate was verified.

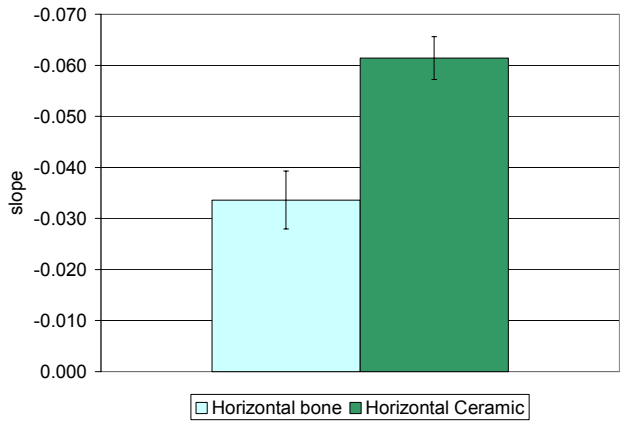

Figure 23 Fracture rate(*b*-value) for horizontally oriented groups

When the *a*-value, productivity, was evaluated no statistical difference was found(p=.48) .Figure 24 shows that the *a*-value for the ceramic is higher that the bone.

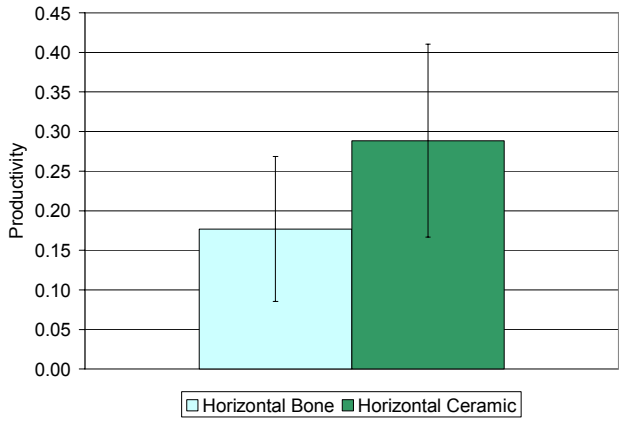

Figure 24: Productivity(*a*-value) for horizontally oriented groups

4.1.2.b Maximum Amplitude, Average Amplitude, Cumulative Events (Semi-quantitative)

The horizontal ceramic had a higher maximum amplitude than the horizontal bone. There was no statistical trend or difference between the groups(p=.65) as shown in Figure25

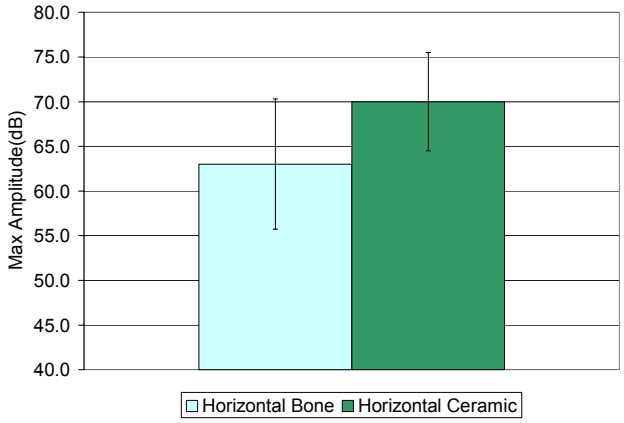

Figure 25 Maximum amplitude for horizontally oriented groups

The average amplitude was statistically different when comparing the horizontal bone and ceramic(p=.04). Figure 26 shows that the average amplitude for the was higher for the bone specimens. The results show that the average amplitude was higher in the comparison of vertical bone to vertical ceramic and horizontal bone to horizontal ceramic. An explanation is that the ceramics generated more events and those events had a low magnitude. This would explain why the ceramics have a higher maximum magnitude but lower average magnitude.

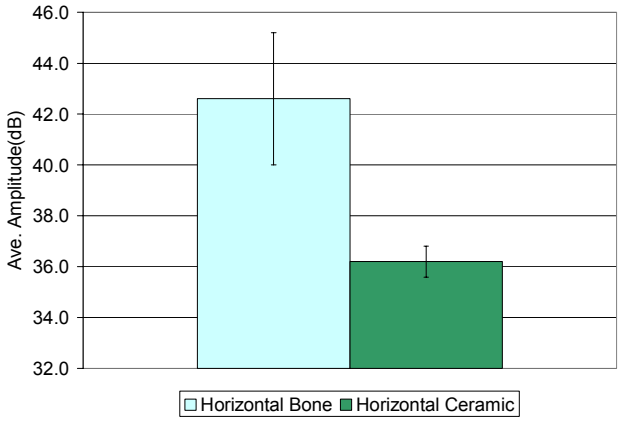

Figure 26: Average amplitude of horizontally oriented groups

The validity of why a lower average magnitude for the horizontal ceramic is dependent upon the horizontal ceramic recording more events than the horizontal bone. Figure27 shows that the horizontal ceramic is a magnitude of order higher than the horizontal bone(p=.0032). The disparity was not was high as the comparison of vertical bone to vertical ceramic, but the difference in material was the strongest contributing factor.

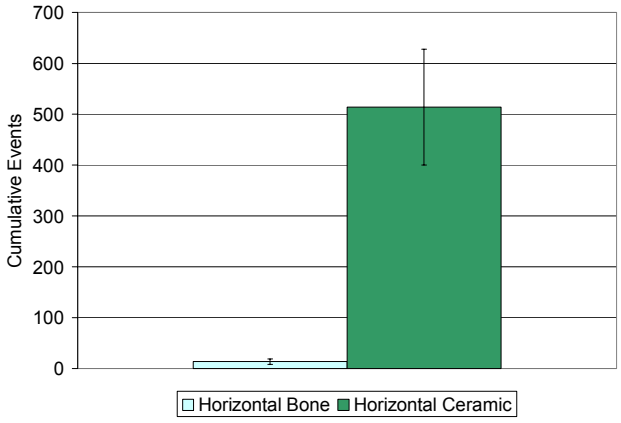

Figure 27: Cumulative events for horizontally oriented groups

The comparison of groups with direction material and different material was used to address the first specific aim. The first aim's hypothesis was that the Gutenberg Richter would be able to differentiate the materials direction by statistically different *a*-

values and *b*-values. The hypothesis was partially correct because only the *a*-value comparing the horizontal direction showed a statistical significance.

4.2.1 Specific Aim 2 (Ceramics)

The second specific aim was to investigate the effect of direction. The hypothesis for the second aim asserted that the Gutenberg-Richter parameters would be statistically different for the directions. The analysis evaluated the groups comprised of the same material and different structural orientation. As discussed in the methodology chapter, the ceramic groups were tested first because the ceramics had arranged struts and homogeneous chemical composition, which limited variability.

4.2.1.a Gutenberg Richter (Quantitative)

Figure28 shows the mean value of the *b*-values; the figure shows that the horizontal ceramic had a higher *b*-value than the vertical ceramic. The horizontal ceramic was anticipated to have a higher *b*-value because it is structurally weaker as shown in Table 2.[(Aue 1998) The *b*-value was not found to be statistically different for the two groups(p=.31).

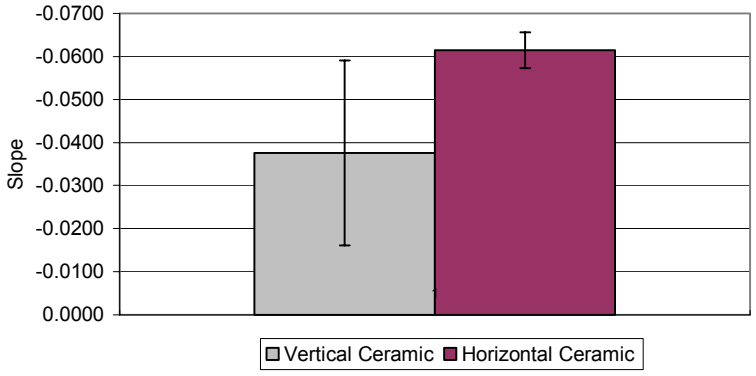

Figure 28: Mean fracture rate(*b*-Value) for ceramic groups

Figure 29 indicates that the horizontally oriented ceramic had the higher *a*-value. There is a lack of a statistical difference in direction for the *a*-value(p=.39). The vertical group was lower.

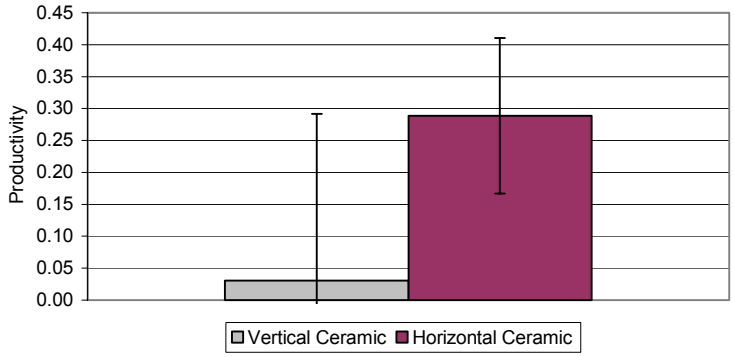

Figure 29: Productivity(*a*-value) for ceramic groups

4.2.1.b Maximum Amplitude, Average Amplitude, Cumulative Events (Semi-quantitative)

Figure30 shows the maximum amplitude for the ceramics. The vertical ceramic had a maximum magnitude of 74.7 dB as compared to 68.9 dB for the horizontal ceramic. The 6 dB difference was not significant(p=.46).

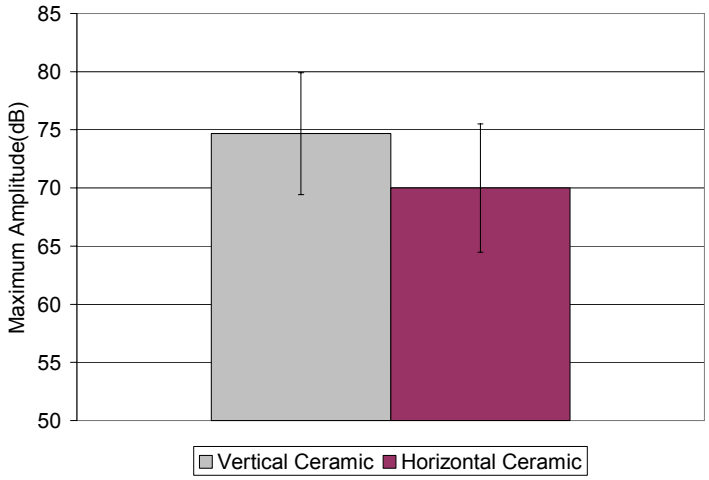

Figure 30 Maximum amplitude for ceramic groups

After comparing the maximum amplitude, the average amplitude and cumulative events were compared. Figure 31 shows the mean values of the average amplitude. The horizontal ceramic is higher by 1 dB. There was no statistical difference or trend(p=.17)

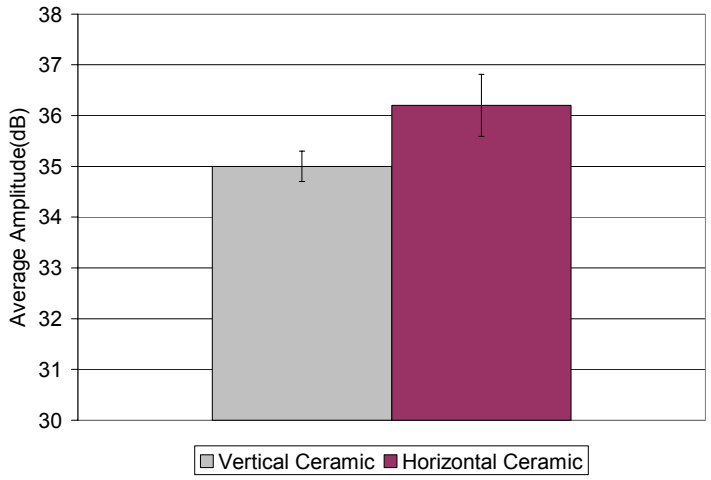

Figure 31 Average amplitude for ceramic groups

The cumulative number of events was an indicator for direction for the ceramics. Figure 32 shows that the ceramic group exhibit a strong statistical difference(p=.016).

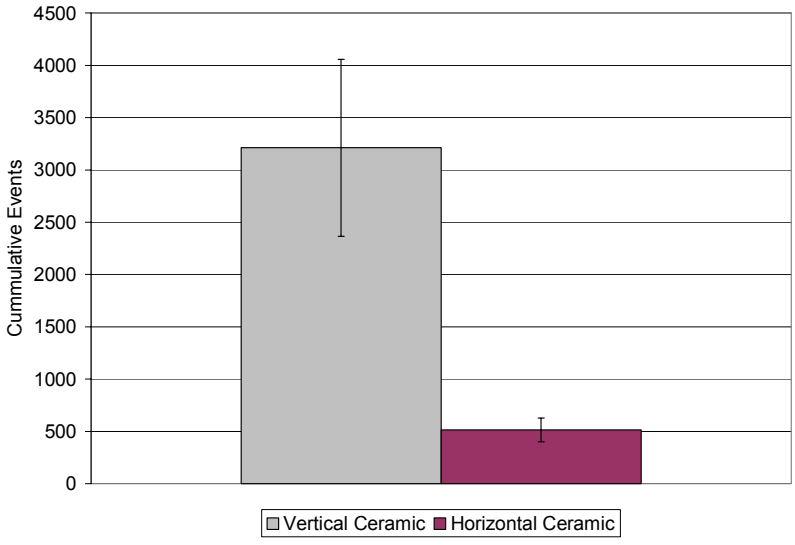

Figure 32: Pre-Fracture cumulative events for ceramics

MicroCT analysis indicated that the vertical and horizontal ceramic specimens have the same bone to volume ratio(porosity). This implies that there is the same amount of a matter in the same volume. The statistical difference in the events is explained by the difference in structural orientation. As shown in Figure 33, the oval surrounds struts that separate two levels, which shows where the horizontal specimens failed.

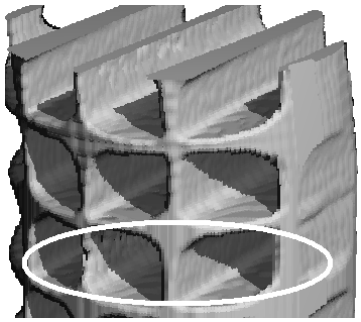

Figure 33: MicroCT image indicating the failure location of the horizontal specimens

Once a load exceeded the failure strength of the struts, the horizontal sample failed. The horizontal specimens failed at a mean value of 83.3 seconds, while the vertical specimens failed at 237.3 seconds. The stress/strain graphs of the vertically oriented ceramics were more complex than the horizontally oriented specimens.

Figure 33 is a representative of the failure pattern for a horizontal and vertical specimens. The successive peaks were assumed to be caused by successive vertical strut failure until ultimate failure.

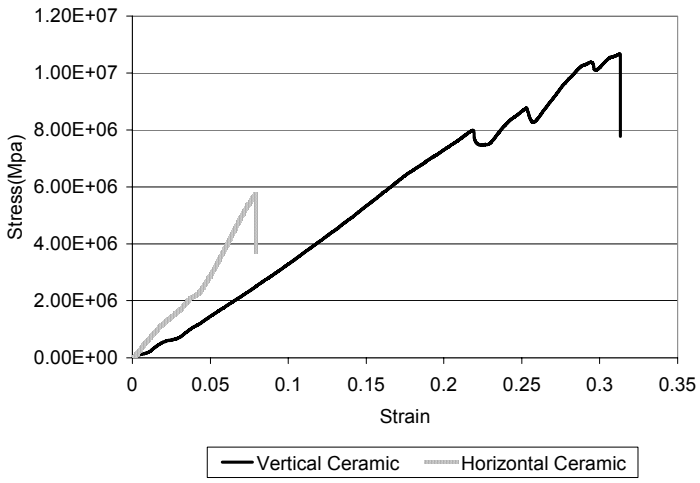

Figure 34 Representative stress/strain graphs for horizontal and vertical ceramic specimens

An additional source of variability for the ceramics was caused by the extraction process. The samples in these tests were machined using a trephine(circular saw). On a block of the sample, the brittle nature of the ceramics made machining difficult. Figure35 is an example of a specimen extracted for a vertically oriented sample. The figure shows that there are imperfections when compared to Figure15.

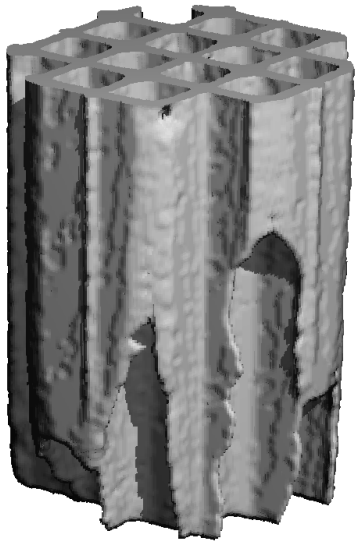

Figure 35: Microcomputer tomography image showing partially damaged vertically oriented Ceramic

The machining process causes an increase in specimen variability because the imperfections did not appear consistently in every sample. In the case of the horizontal oriented ceramics, machining produced samples with fewer imperfections than the vertical specimens. The micro-damage on the vertical specimens was on the periphery, so the structural integrity was not compromised. Overall, the machine-induced imperfections did not cause a contradiction for the assumption that the vertically oriented specimens would have a lower *b*-value and higher *a*-value. The imperfections affected the events recorded because the defects produced stress concentrations. The micro-damage resulted in event detection, which altered *b*-value results.

The *b*-value and *a*-value for the ceramic groups did exhibit explainable physical correlations even though they could not be statistically verified as different. The next step was to run the analysis on bovine specimens. In using bovine specimens, material factors such as porosity(texture) would have an impact on the results.

4.2.2 Specific Aim 2 (Bone)

4.2.2.a Gutenberg Richter (Quantitative)

The b-value for the two bone groups is displayed on Figure 36. The vertical bone has a higher average when comparing the two groups. Again, the statistical test indicated that there was no difference between these two groups(p=.25).

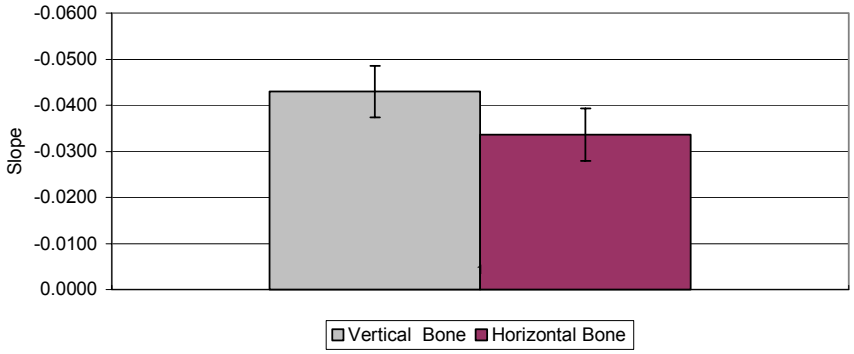

Figure 36: Fracture rate(*b*-value) for bone groups

However, just as in the case of the ceramics, the actual fracture pattern between the two groups exhibited different characteristics in the pre-yield region, the horizontal bone yielded on an average 12 seconds at a .01mm/s strain rate. The vertically aligned trabecular specimens failed on average of 145 seconds at the same rate. The vertical specimens yielded at higher stress values and strain values than the horizontal specimens. Also, the horizontal specimens had a sample size of n=6 and the vertical had a sample of n=9. The horizontal sample size was smaller because 4 tests yielded no preyield events and all of the events recorded were well into the plastic region nearing failure.

The higher b-value average for the vertically oriented bone can possibly be explained by its viscoelastic mechanical properties. Viscoelasticity implies that the mechanical properties are a function of the rate of the applied load. According to the literature, the rate of .01mm/s is a high rate. Higher rates cause viscoelastic materials to function more like brittle materials. The trabecular bone was stiffer in vertical direction. The higher *b*-value for the vertical bone contradicts the trend that the weaker specimen should have the higher b-value. When characterizing bone, the heterogeneous composition and variable structure have a strong impact on the resulting acoustic emission as discussed in Chapter 1. The trabecular struts were not as directionally aligned as the ceramic specimens.

Micro-CT analysis did indicate that the samples had a lower bone volume fraction in the horizontal direction, so the varying porosity between bone samples was also a factor. The fracture mechanisms induced could not be simplified to the trend that would characterize the ceramics.

The a-value of the trabecular bone was higher in the horizontal direction. Figure 35 shows the direction of the horizontal trabecular bone.

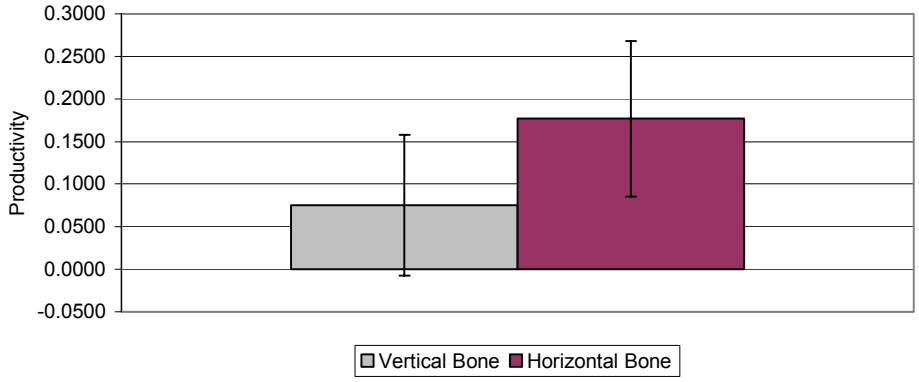

Figure 37: Productivity(*a*-value) for bone groups

The *a*-value results did not result in statistically significant difference(p=.43). The *a*-value result is the same as the ceramics because the vertically oriented ceramics had the lowerr *a*-value than the horizontally oriented ceramics.

4.2.2.b Maximum Amplitude, Average Amplitude, Cumulative Events (Semi-quantitative)

Figure 38 shows that the maximum event amplitude for horizontally oriented trabecular bone was 64.8 dB compared to 57.1 dB for vertically oriented trabecular bone. The difference was not significant(p value=.46)

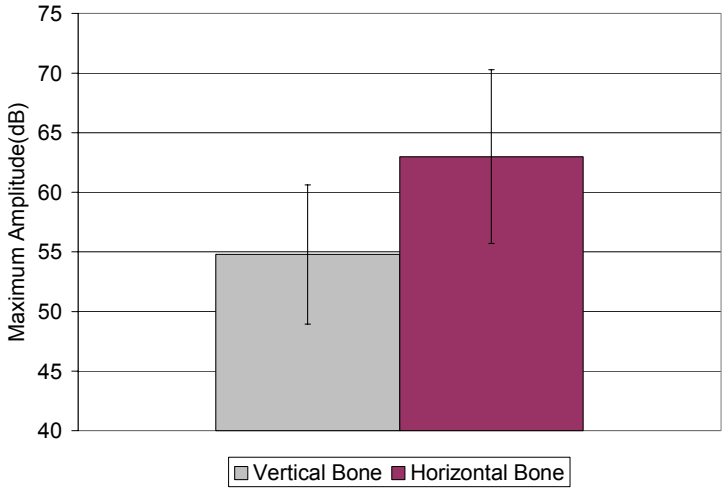

Figure 38: Maximum amplitude for bone groups

The average amplitude showed a statistical trend of results(p=.07). Figure 39 shows the mean value for the average amplitude for trabecular specimens

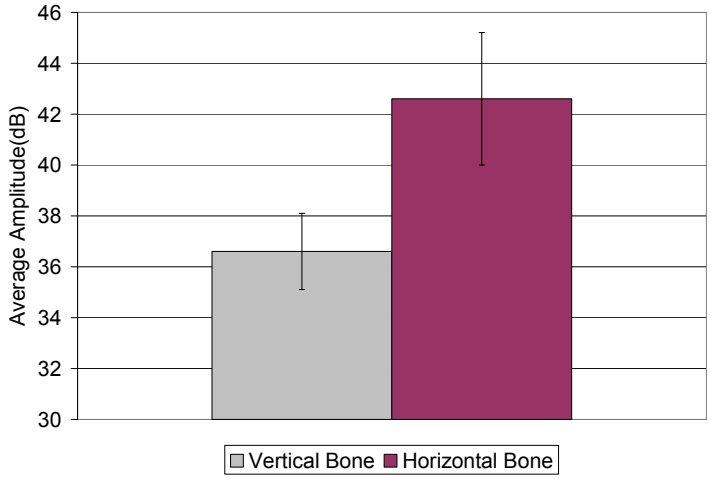

Figure 39: Average amplitude for bone groups

Figure 40 shows that the cumulative events of the bone specimens did not exhibit a statistical difference(p=.87). The cumulative events differ by less than one which suggested that the bone yields in the same fashion.

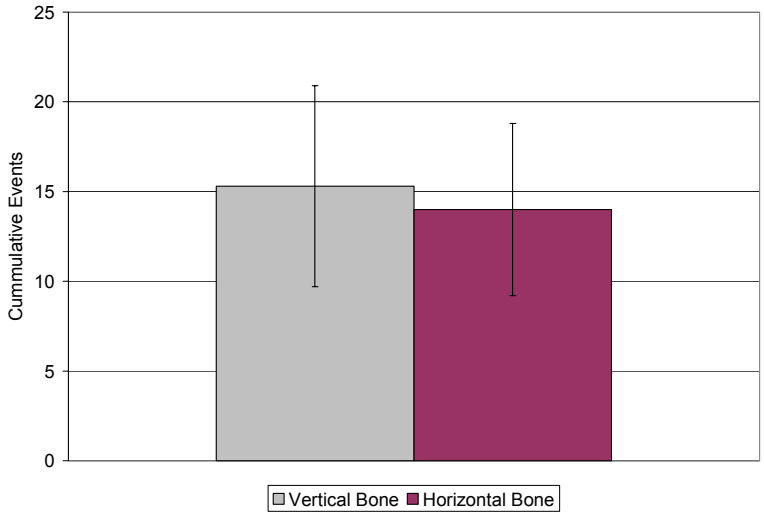

Figure 40:Pre-yield cumulative events for bone groups

The comparison of groups with same material and different direction was used to address the second specific aim. The second aim's hypothesis was that the Gutenberg Richter would be able to differentiate the materials direction by statistically different *a*-values and *b*-values. The hypothesis was shown to be false; the GR-relationship could not show a difference.

4.3 Specific Aim 3 (Micro-damage)

The third specific aim wanted to determine if acoustic emission could verify that there is damage in the pre-yield region. The last experiment was the histology test; during the test, the number of events were correlated to visual slides prepared from specimens after being mechanically tested. In order to monitor the sample effectively in the elastic region, the strain rate was reduced to .001mm/s from .01 mm/s. A 2% strain for the specimens ranged from .12 to .2 mm. The displacement distance was very small and is exceeded in the previous tests with in 5 to 10 seconds. Due to the variance in strength for each sample, the higher strain rate would have made keeping a sample in the pre-yield

region more difficult. The staining in the histology study would have indicated damage that did not occur in the pre yield region because there was greater chance that the test could not have been stopped pre-yield.

Three samples were tested in both directions at the lower strain rate. Minimal acoustic emission events were detected in the tests. The histology study did not provide sufficient results in terms of acoustic emission. The results from the histology study also indicated that there was minimal trabeculi damage when viewing the slides. The damage was indicated by green markings on the trabeculi while using the florescent microscope. In viewing all of the slides, most of the damage was indicated on the periphery of the samples.

The damage on the side of the sample was not a true indicator of failure because the damage could have been caused by handling, in addition to the mechanical testing. Another difficulty in capturing acoustic events is the fact that the specimens were de-marrowed to aid the setting of the fluorescent dyes in the sample. The presence of marrow has a positive effect on the propagation of events for acoustic emssion. So, a histology study that attempts to link the acoustic emission events will be negatively affected by the necessity to demarrow the specimens.

Figure41 and 42 are digital images of specimens from the histology test. Figure 41 shows a horizontally oriented specimen with no damage. Figure 42 is one of the vertically oriented samples that show some damage. This particular specimen yielded under the compressive stress. In comparing the vertically and horizontally oriented samples, the periphery of the vertical samples exhibited more damage because machining weakened the trabeculi along the direction; the ensuing compressive testing increase the

damage. Figure 42 shows a magnified section of bright green area in the center of the figure. The area is a chemical indication of exposed calcium after the sample was mechanically tested. The calcium was exposed due to damage of the trabecular strut. The image is characterized as damage because it is in the center of the trabeculi. A fracture would have been a green line across the width of the trabecular strut.

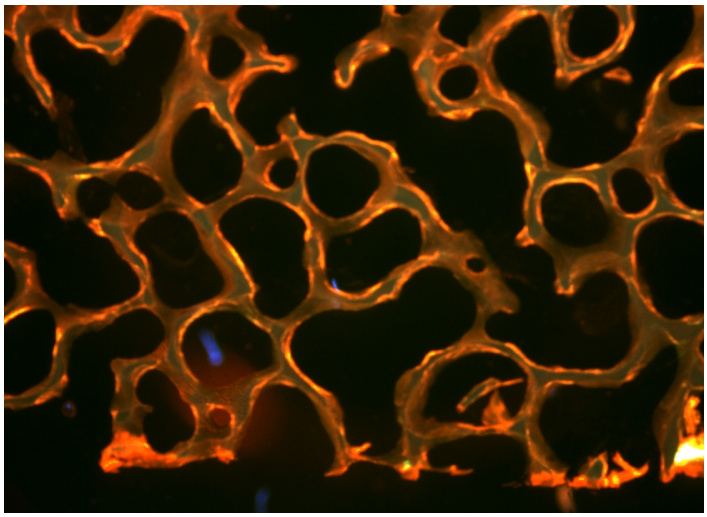

Figure 41: Horizontally oriented sample indicating no damage thorough fluorescence.

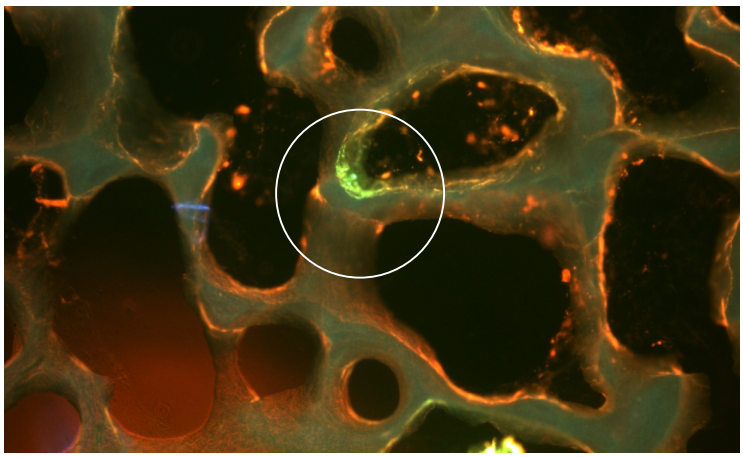

Figure 42: Magnified Vertically oriented sample indicating damage thorough fluorescence.

The histology study showed a minimal difference between the orientations. The stress-strain information indicates that the material was deforming but minimal hits were detected. The slower strain rate used to complete the mechanical testing may have affected the acoustic emission and these events may not have been detected. A previous study found that slower strain rates induce lower amplitude events.(Fischer 1986)

The third specific aim wanted to address AE capabilities to detect damage and fracture. The hypothesis was asserted that acoustic emission could detect damage. The hypothesis was shown to be in false. The acoustic emission setup recorded a total of 5 events over all 6 mechanically tested sample. The histology study indicated that there is damage but not failure of the struts. The deforming sample and no detectable hits imply that the system was not sensitive enough to detect damage events.

.

CHAPTER 5 CONCLUSION

The purpose of this study was to evaluate if a seismic power law post processing technique could be used to differentiate the structural orientation of trabecular bone. The trabecular bone specimens were tested to learn more about the yield and fracture characteristics. The study anticipated that the fracture distributions detected by acoustic emission would also display the differences in bone cut in the vertical(inferior-superior) and horizontal(medial-lateral) direction. The histology study was used to increase correlations between micro-damage, micro-fracture and the acoustic emission response. Tests were run to determine the effectiveness of the Gutenberg Richter relationship. After the GR parameters were calculated and compared, the semi-quantitative relationships(maximum amplitude, average amplitude and cumulative events) were evaluated.

5.1 Specific Aim 1

5.1.1Specfic Aim 1(vertical)

The first specific aim wanted to evaluate if the GR relationship could differentiate bone and ceramic groups with the same structural orientation. The GR parameters for the vertical group indicated that there were no statistical difference between the vertical bone and vertical ceramic, thus the hypothesis was proven false. The vertical bone had a higher fracture rate and productivity than the vertical ceramic. The bone had a higher fracture rate because, which is attributed to it being a weaker material.(Aue 1998)

When the maximum amplitude, average amplitude and cumulative events were compared, the maximum amplitude and cumulative events showed a statistical difference. The maximum amplitude was higher for the ceramics. The average amplitude was higher for the bone. Since the ceramics recorded significantly more events and with low amplitude, the results indicated that the bone had a higher average amplitude.

5.1.2 Specific Aim 1 (horizontal)

Evaluating the GR parameters in the horizontal direction was a partial success. The *a*-value showed no difference, but the *b*-value was significantly different. Both materials were weaker in the horizontal direction in comparison to the vertical direction for their respective material groups.

When the maximum amplitude, average amplitude and cumulative events were compared, the average amplitude and cumulative events showed a statistical difference. A higher average amplitude for bone and higher cumulative event for ceramic was the same trend as the vertical ceramic and vertical bone.

5.2 Specific Aim 2

5.2.1 Specifc Aim 2 (Ceramic)

The second specific aim wanted to evaluate if the GR relationship could differentiate vertically and horizontally oriented groups of the same material. Ceramic groups were tested first due to decreased variability in orientation and chemical composition. The GR relationship could not statistically differentiate the *b*-value or *a*-value of vertically and horizontally oriented ceramics. The vertical ceramic resulted in a

lower *b*-value and lowerr *a*-value than the horizontal ceramic. The ceramics exhibited results that could be explained by their structural composition.(Aue 1998)

The maximum amplitude, average amplitude and cumulative events were compared. There was no statistical difference between the average and maximum amplitude. This implied that when the ceramic strut fractured that the energy released may have been caused by the same fracture mechanisms over the duration of the test. The cumulative events were significantly higher for the vertical ceramic because of the lower times in which the horizontal specimens failed and the orientation of the horizontal specimen.

5.2.2 Specific Aim 2(Bone)

The seismic power-law could not distinctively differentiate direction of trabecular strut orientation. The study showed that the hypothesis was proven false. The b-value was higher for the vertically oriented direction because the bone was thicker and possessed more struts along the vertical direction; the fracture rate was increased because there was physically more matter to fracture in the vertical direction. The a-value was higher for the horizontally oriented direction. Overall, the parameters for the Gutenberg Richter-relationship was not indicative of trabecular direction orientation. The hypothesis was proven to be false.

The variability between each sample and the structural properties of trabecular bone were the strongest factors affecting the statistical results. In the case of the trabecular specimens, the porosity is directly tied to the orientation because the principal loading direction causes the samples to be thicker in that direction.

The maximum amplitude, average amplitude and cumulative events were compared. There was no difference in any of the relationships. However, the fact that the cumulative events differed by less that 1 indicated that there may be similar yield mechanisms which are independent of direction.

5.3 Specific Aim 3

The motivation of the third specific aim was to determine if the acoustic emission could be used to indicate damage in the pre-yield region. A histology study was used to compare the loading damage to the acoustic emission response. The histology study showed that samples cut in the vertical direction exhibited more damage than the horizontal samples. The study did not verify any trends for the acoustic emission because only one of the samples induced any hits; the sample totaled 4 hits in the elastic region. Less damage was seen in the horizontal samples because the orientation of these struts were not as stiff as the vertically oriented samples. Once the specimens were unloaded, the trabecular struts exhibited minimal damage on the micro-structural level. The strain rate was altered to insure that the specimens were loaded only in the elastic regions.

There are two reasons for the lack of acoustic emission events, the change in strain rate and sensitivity of the equipment. The sensitivity issue was important because the mechanical testing data indicated that the events did occur, However, the sensitivity of the transducers was not precise enough to capture the low amplitude events created by the initial of micro-damage.

5.4 Issues and Future Study

The study showed that The GR relation ship could not be used to differentiate direction. The results for the vertical ceramic did show that the calculation of the a-value can be skewed by b-value variability and high maximum amplitude. These occurrences seriously affect the physical significance and interpretation of the productivity.

The preliminary research did broach the issue of the Omori's law. The development of using the power law analysis has the option of using Omori's law to analyze the rate of decay for single event. The patterns developed from characterizing a single event are anticipated to be more insightful. The option of Omori's law development as a post processing technique appears to be a viable option. The option can be explored once the software and processing speeds can match the requirements of the decaying events.

Another change that should be evaluated is a change in testing mode. The previous studies placed their specimen under three point bending and tension. Changing the testing directions will alter the fracture patterns because of the change in stress on trabeculi. The use of end caps and there effect was not discussed in previous studies. The study at hand found that the use of end caps had an effect on the events recorded. The platen/specimen interaction caused events because the specimens had peripheral damage due to the extraction process, so a change in test direction must account for the end-caps.

As techniques and software evolve, an experiment that induces solely friction events can be distinguished by frequency content. It is extremely important that acoustic emission be able to determine the difference between micro-damage and micro-fracture. Acoustic emission experiments must be related to yield and friction because these cause micro-damage. Friction of sliding trabecular struts is less understood than fracture phenomenon of trabecular struts.

The study indirectly found that the GR relationship can be determined to find a difference in porosity and material. The next step would have been used to involve human specimens. The GR relationship could not be used to determine the orientation of trabecular bone of bovine specimens. The acoustic emission alone did exhibit marginal success in differentiating mater it could be used to find the differences in types of materials. The productivity and fracture rate values for bovine, human and osteoportic human bone should be evaluated statistically.

APPENDIX

APPENDIX A: STATISTICAL RESULTS

Table:3 Mean value of GR Parameters, Acoustic emission indicators and mechanical testing data

	Mean	**Std. Dev.**	**Std. Error**
Fracture rate(b-value)			
vertical bone	-0.0430	0.01685	0.0056
horizontal bone	-0.0336	0.01321	0.0057
vertical ceramic	-0.0376	0.06460	0.0215
horizontal ceramic	-0.0614	0.01248	0.0042
Produtivity (a-value)			
vertical bone	0.0750	0.24770	0.0826
horizontal bone	0.1768	0.22420	0.0915
vertical ceramic	0.0310	0.78800	0.2600
horizontal ceramic	0.2886	0.36600	0.1220
Cumulative Events			
vertical bone	15.3	13.5	4.8
horizontal bone	14	13.7	5.6
vertical ceramic	3212	2391	846
horizontal ceramic	514	323	114
Maximum Amplitude			
vertical bone	54.8	17.48	5.83
horizontal bone	63.0	17.82	7.28
vertical ceramic	74.7	15.71	5.24
horizontal ceramic	70.0	16.57	5.52
Average Amplitude			
vertical bone	36.6	4.49	1.5
horizontal bone	42.6	7.24	2.6
vertical ceramic	35.0	0.90	0.3
horizontal ceramic	36.2	1.82	0.61
Modulus			
vertical bone	66.3	25.90	8.6
horizontal bone	41.3	14.90	4.7
vertical ceramic	83.3	49.30	16
horizontal ceramic	81.8	35.30	12
Strength			
vertical bone	9.1	4.33	1.4
horizontal bone	3.8	1.51	0.48
vertical ceramic	12.6	5.04	1.7
horizontal ceramic	5.4	2.50	0.89

Minitab Student T-test results 95% Confidence level

Key

Vertical bone average amplitude	vbavamp
Vertical bone maximum amplitude	vbmaxamp
Vertical bone b-value	vbbval
Vertical bone a-value	vbaval
Vertical bone cumulative events	vbevents
Horizontal bone average amplitude	hbavamp
Horizontal bone maximum amplitude	hbmaxamp
Horizontal bone b-value	hbbval
Horizontal bone a-value	hbaval
Horizontal bone cumulative events	hbevents
Vertical ceramic average amplitude	vcavamp
Vertical ceramic maximum amplitude	vcmaxamp
Vertical ceramic b-value	vcbval
Vertical ceramic a-value	vcaval
Vertical ceramic cumulative events	vcevents
Horizontal ceramic average amplitude	hcavamp
Horizontal ceramic maximum amplitude	hcmaxamp
Horizontal ceramic b-value	hcbval
Horizontal ceramic a-value	hcaval
Horizontal ceramic cumulative events	hcevents

Two Sample T-Test and Confidence Interval

```
Two sample T for vbmaxamp vs hbmaxamp

           N      Mean     StDev   SE Mean
vbmaxamp   9      57.1      17.1       5.7
hbmaxamp   8      64.8      19.9       7.0

95% CI for mu vbmaxamp - mu hbmaxamp: ( -27.2,  11.9)
T-Test mu vbmaxamp = mu hbmaxamp (vs not =): T = -0.84  P = 0.41  DF =
13
```

Two Sample T-Test and Confidence Interval

```
Two sample T for vbavamp vs hbavamp

          N      Mean     StDev   SE Mean
vbavamp   9     36.66      4.49       1.5
hbavamp   8     42.64      7.24       2.6

95% CI for mu vbavamp - mu hbavamp: ( -12.5,  0.5)
T-Test mu vbavamp = mu hbavamp (vs not =): T = -2.02  P = 0.069  DF =
11
```

Two Sample T-Test and Confidence Interval

```
Two sample T for hbbval vs vbbval

        N      Mean     StDev   SE Mean
hbbval  6   -0.0336    0.0132    0.0054
vbbval  9   -0.0430    0.0168    0.0056

95% CI for mu hbbval - mu vbbval: ( -0.0076,  0.0263)
T-Test mu hbbval = mu vbbval (vs not =): T = 1.21  P = 0.25  DF = 12
```

Two Sample T-Test and Confidence Interval

```
Two sample T for hbaval vs vbaval

        N      Mean     StDev   SE Mean
hbaval  6     0.177     0.224     0.092
vbaval  9     0.075     0.248     0.083

95% CI for mu hbaval - mu vbaval: ( -0.170,  0.373)
T-Test mu hbaval = mu vbaval (vs not =): T = 0.83  P = 0.43  DF = 11
```

Two Sample T-Test and Confidence Interval

```
Two sample T for vcavamp vs hcavamp

         N      Mean     StDev   SE Mean
vcavamp  9    35.180     0.903      0.30
hcavamp  9     36.17      1.82      0.61

95% CI for mu vcavamp - mu hcavamp: ( -2.48,  0.50)
T-Test mu vcavamp = mu hcavamp (vs not =): T = -1.46  P = 0.17  DF = 11
```

Two Sample T-Test and Confidence Interval

```
Two sample T for vcmaxamp vs hcmaxamp

          N      Mean     StDev   SE Mean
vcmaxamp  9      74.7      15.7       5.2
hcmaxamp  9      68.9      16.6       5.5

95% CI for mu vcmaxamp - mu hcmaxamp: ( -10.4,  22.0)
T-Test mu vcmaxamp = mu hcmaxamp (vs not =): T = 0.76  P = 0.46  DF =
15
```

Two Sample T-Test and Confidence Interval

```
Two sample T for hcbval vs vcbval
```

```
        N      Mean     StDev   SE Mean
hcbval  9   -0.0614    0.0125    0.0042
vcbval  9   -0.0376    0.0646     0.022

95% CI for mu hcbval - mu vcbval: ( -0.0744,  0.027)
T-Test mu hcbval = mu vcbval (vs not =): T = -1.09  P = 0.31  DF = 8
```

Two Sample T-Test and Confidence Interval

```
Two sample T for vcaval vs hcaval

        N      Mean     StDev   SE Mean
vcaval  9     0.031     0.788      0.26
hcaval  9     0.289     0.366      0.12

95% CI for mu vcaval - mu hcaval: ( -0.89,  0.38)
T-Test mu vcaval = mu hcaval (vs not =): T = -0.89  P = 0.39  DF = 11
```

Two Sample T-Test and Confidence Interval

```
Two sample T for vbavamp vs vcavamp

         N      Mean     StDev   SE Mean
vbavamp  9     36.66      4.49       1.5
vcavamp  9    35.180     0.903      0.30

95% CI for mu vbavamp - mu vcavamp: ( -2.0,  5.00)
T-Test mu vbavamp = mu vcavamp (vs not =): T = 0.97  P = 0.36  DF = 8
```

Two Sample T-Test and Confidence Interval

```
Two sample T for vbmaxamp vs vcmaxamp

          N      Mean     StDev   SE Mean
vbmaxamp  9      57.1      17.1       5.7
vcmaxamp  9      74.7      15.7       5.2

95% CI for mu vbmaxamp - mu vcmaxamp: ( -34.1,  -1.1)
T-Test mu vbmaxamp = mu vcmaxamp (vs not =): T = -2.27  P = 0.039  DF =
15
```

Two Sample T-Test and Confidence Interval

```
Two sample T for vcbval vs vbbval

        N      Mean     StDev   SE Mean
vcbval  9   -0.0376    0.0646     0.022
```

```
vbbval  9   -0.0430    0.0168    0.0056

95% CI for mu vcbval - mu vbbval: ( -0.045,  0.0557)
T-Test mu vcbval = mu vbbval (vs not =): T = 0.24  P = 0.81  DF = 9
```

Two Sample T-Test and Confidence Interval

```
Two sample T for vcaval vs vbaval

        N      Mean     StDev   SE Mean
vcaval  9     0.031     0.788      0.26
vbaval  9     0.075     0.248     0.083

95% CI for mu vcaval - mu vbaval: ( -0.67,  0.579)
T-Test mu vcaval = mu vbaval (vs not =): T = -0.16  P = 0.88  DF = 9
```

Two Sample T-Test and Confidence Interval

```
Two sample T for hcmaxamp vs hbmaxamp

          N      Mean     StDev   SE Mean
hcmaxamp  9      68.9      16.6       5.5
hbmaxamp  8      64.8      19.9       7.0

95% CI for mu hcmaxamp - mu hbmaxamp: ( -15.2,  23.5)
T-Test mu hcmaxamp = mu hbmaxamp (vs not =): T = 0.46  P = 0.65  DF =
13
```

Two Sample T-Test and Confidence Interval

```
Two sample T for hbavamp vs hcavamp

         N      Mean     StDev   SE Mean
hbavamp  8     42.64      7.24       2.6
hcavamp  9     36.17      1.82      0.61

95% CI for mu hbavamp - mu hcavamp: ( 0.2,  12.69)
T-Test mu hbavamp = mu hcavamp (vs not =): T = 2.46  P = 0.043  DF = 7
```

Two Sample T-Test and Confidence Interval

```
Two sample T for hcbval vs hbbval

        N      Mean     StDev   SE Mean
hcbval  9   -0.0614    0.0125    0.0042
hbbval  6   -0.0336    0.0132    0.0054

95% CI for mu hcbval - mu hbbval: ( -0.0430,  -0.0126)
T-Test mu hcbval = mu hbbval (vs not =): T = -4.08  P = 0.0022  DF = 10
```

Two Sample T-Test and Confidence Interval

```
Two sample T for hbaval vs hcaval

        N      Mean     StDev   SE Mean
hbaval  6     0.177     0.224     0.092
hcaval  9     0.289     0.366      0.12

95% CI for mu hbaval - mu hcaval: ( -0.444,  0.22)
T-Test mu hbaval = mu hcaval (vs not =): T = -0.73  P = 0.48  DF = 12



Worksheet size: 100000 cells
Retrieving project from file:
C:\DOCUME~1\ADMINI~1\DESKTOP\MSTHES~1\AETEST.MPJ
```

Two Sample T-Test and Confidence Interval

```
Two sample T for vbevents vs hbevents

          N      Mean     StDev   SE Mean
vbevents  8      15.3      13.5       4.8
hbevents  6      14.0      13.7       5.6

95% CI for mu vbevents - mu hbevents: ( -15.1,  17.6)
T-Test mu vbevents = mu hbevents (vs not =): T = 0.17  P = 0.87  DF =
10
```

Two Sample T-Test and Confidence Interval

```
Two sample T for vcevents vs hcevents

          N      Mean     StDev   SE Mean
vcevents  8      3212      2391       846
hcevents  8       514       323       114

95% CI for mu vcevents - mu hcevents: ( 679,  4717)
T-Test mu vcevents = mu hcevents (vs not =): T = 3.16  P = 0.016  DF =
7
```

Two Sample T-Test and Confidence Interval

```
Two sample T for vbevents vs vcevents

          N      Mean     StDev   SE Mean
vbevents  8      15.3      13.5       4.8
```

```
vcevents  8      3212      2391       846

95% CI for mu vbevents - mu vcevents: ( -5197.6,  -1196)
T-Test mu vbevents = mu vcevents (vs not =): T = -3.78  P = 0.0069  DF
= 7
```

Two Sample T-Test and Confidence Interval

```
Two sample T for hbevents vs hcevents

          N      Mean     StDev   SE Mean
hbevents  6      14.0      13.7       5.6
hcevents  8       514       323       114

95% CI for mu hbevents - mu hcevents: ( -770.5,  -230)
T-Test mu hbevents = mu hcevents (vs not =): T = -4.38  P = 0.0032  DF
= 7
```

APPENDIX B EXTRACTION PROTOCOL

Bovine Specimen Extraction

Materials

Bone(Bovine Fibia or Tibia)
Mixing Cups(Preferably Disposable and Metric)
Duct tape
Epoxy(Currently use Orthojet: Liquid/powder)
PBS(phosphate buffered solution
Sample holders
Drop cloths
Scalpels
Disposable Stirrers
Metal Cylinders(seeNote*)
Oscillating saw
Disposable pipets
Aprons

DAY BEFORE

The specimens are extracted using a oscillating saw/drill(3M). The day prior to any extraction of specimens, the nitrogen tank used to power the drill was checked. If the reading was below 500 psi., the tank was replaced. The saw was also checked to see if it was in working order. The bovine bone was also taken out of the freezer and placed in a refrigerator to initiate the defrosting process. Four hours before the specimens are extracted, the bone was taken out of the refrigerator to achieve room temperature. The final thawing process made it less difficult to clear the soft tissue away from the bone.

EXTRACTION DAY

Area Preparation

The extraction of the bone specimens caused the splatter of much soft tissue debris. Proper protection and sanitation measures were taken due to biohazard risks. Upon entering the preparation area, gloves, eyewear, aprons and foot wear were worn. Also, drop clothes were placed to prevent splattering of tissue and ease cleanup.

Bone Preparation

The bone preparation began with cleaning all muscle and soft tissue from the ends of the bone. After the bone was cleared of flesh, the aluminum cylindrical shells were used to mark where the bone would be cut. The oscillating saw was used to cut the bone. The region were the cut was made was the diaphyis (long shaft) of the femur. Once the cut was made the two pieces of bone were set aside. One side of the aluminum cylindrical shell was covered with a tight layer of tape in order to hold the weight of the bone and the cement used to pot the bone. At this point, either the distal end of the femur or proximal end of the tibia is placed in to the cylinder, depending on which end samples are desired. The next step involved mixing the fast curing dental cement.

The cement is comprised of two portions Orthojet liquid and Orthojet powder(Lang Dental). One hundred twenty milliliters of solution and 270 milliliter of powder were mixed together. The mixture was quickly poured in the cylinder around the bone. The freshly potted bone was set in a fume hood to capture the scent form the curing cement.

CORING

An hour after the cement has cured, the oscillating saw to cut off the thin layer of cortical bone from the top of the bone to expose the trabecular bone. A six millimeter diameter trephine, circular saw, was used to core out specimens. The trephine was atttaced to the 3M saw by removing the saw attachment and adding the drill connection. The samples were drilled vertically along the shaft of the bone. This direction corresponds to the direction of principle loading, so the trabecular struts were aligned along vertical direction. On average 25 to 30 samples were cored from the potted bone.

The samples were finally extracted from the bone by reconnecting the saw attachment and a horizontal incision was made at the same depth as the length of the trephine. Once the specimens were pulled from the bone, their region was noted. The samples were then preserved by wrapping then is paper towels soaked in Phosphate Buffered Solution(PBS). The specimens were then placed in sample holder tubes for later testing.

The second group of bone sample was extracted from the horizontal (medial/lateral) direction. The coring process was altered by cutting sample from the side instead of the top of the cored bone. Figures B.1-6 are graphical images depicting the coring process for trabecular bone in the vertical(inferior/superior) direction. The extraction process of the ceramics was similar to that of the bone. The coring was completed in a machine shop. The same trephine was used but it was connected to a drill press. Once the vertically aligned ceramic was extracted, the ceramic block was rotated 90 degrees, and the specimens were cored out.

Figure B.1: Thawed bovine femur

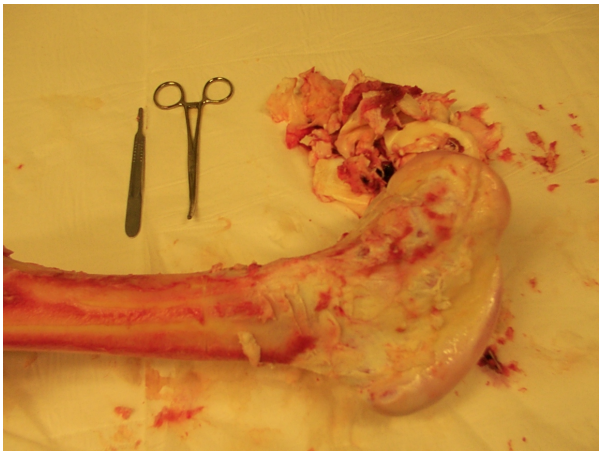

Figure B.2: Cleaned bovine femur

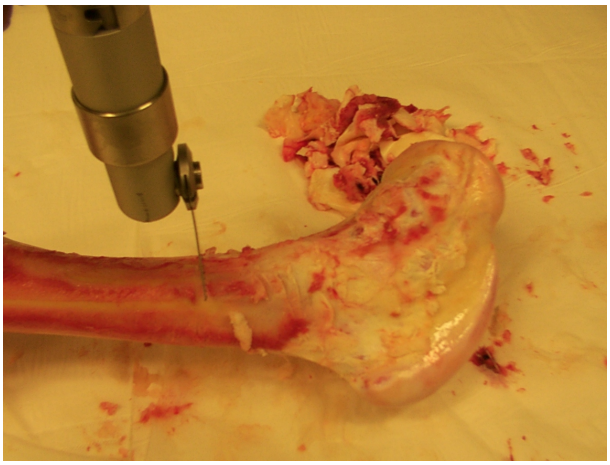

Figure B.3 Sizing and cutting of femur for potting in aluminum cylinder

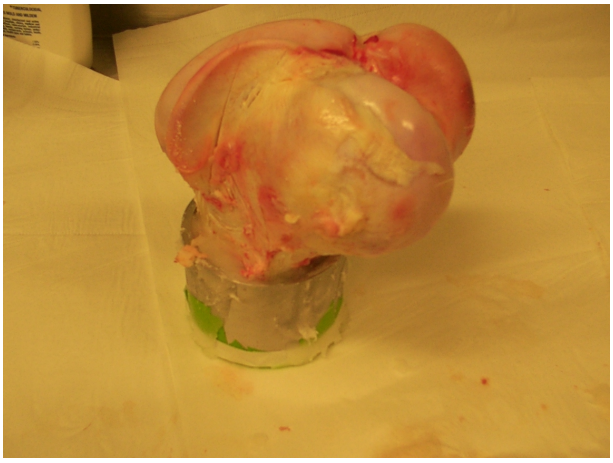

Figure B.4 Potted femur

Figure B.5: Thin cortical bone layer removed to expose trabecular bone

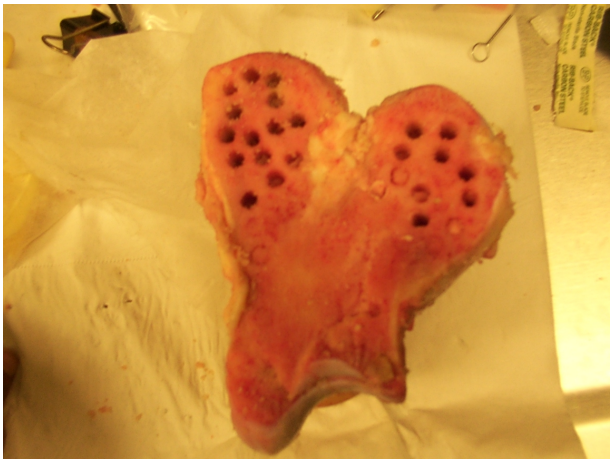

Figure B.6 Specimens extracted using trephine.

APPENDIX C: Matlab Program

```
clear all
close all

%-----------------------------------
%This portion reads in the AE data.
%The file name is the file name used by the file converted
%by the ATASC program.
filename = 'C:\ac\5273vb11.txt';
open(filename)
%the yield time is the time in seconds that the specimen yielded
% after the was Mechanical testing data using the time that the yield
% stress(force) and strain(displacement) was found
yieldtime=120;


%This step turns the test file into the set of columns of data
[T P1 P2 CH R CO E D A] = textread(filename,'%f %f %f %d %d %d %d %d
%d');
%-----------------------------------
%putting each colum into a matrix to be manipulated after the filter
g=[T,P1,P2,CH,R,CO,E,D,A];
%t=time, P1=parametric1, p2=parametric2, ch=channel, R=risetime
%co=counts, E = energy, D=duration, A=amplitude
%When the files were converted from the AE, the headers had to be
%eliminated so the manipulation would be easier
%-----------------------------------
%this portion filters out the Div/0 and Not-a-number
%when creating the a-value. The filter saves the indexes
index=[];

for i=1:size(g(:,1))
   %The first conditional is if the Counts-1=0
   %The second is if the Duration-rise time=0
   %the use of 1 in second condtional insures no divide by 0 in
calculation of a

if (g(i,8)-g(i,5))>1&g(i,1)<(yieldtime+.5)
      %add .5 to include addtional hits that may have been missed
      %save index
      index=[index,i];
   end
end
%crates a nex matrix with filtered data
G=g(index,:);

threshold=[G(:,9)];
for k=1:length(threshold)
   %
   counter=0;
```

```
    %G(:,9) is the column for the  Amplitude
    % The loop counts each time an amplitude occurs
    % and then take the log of it
    %Note: this portion of the code takes the longest
    %it may be optimized.
    %There was a notion that the loop causes it to double
    %count events. There is no double counting of a particular
    %amplitude.  The code treats
    % each number in the column as a separate instance.  This is shown
    %the output 'q'.  When graphing 'q', multiple entries will
    %exist on the same point of the Log(N(w)) vs. Amplitude graph
    for ii=1:size(G(:,9))
       if G(ii,9)>=threshold(k)
          counter=counter+1;
        end
     end
     %b=Log of the occurencs for a magnitude
     b(k)=(log10(counter));
end

%Decieded to add a line to give average amplitude and maxamplitude
aveamplitude=mean(G(:,9))
maxamplitude=max(G(:,9))

figure
plot(threshold,b,'.')
xlabel('Threshold(dB)')
ylabel('b_value')
q=[threshold,transpose(b)]
%writes a text file for to graph in Excell the file will contain 'q'
%column 1 will be the threshold and column 2 will be the Log of the
%occurences
fid =fopen('C:\ac\convert2xl.txt','w');
%the user then needs to change the name of the convert2xl
%for each differnet file.
fprintf(fid,'%4.3f %4.3f\r',q');
status=fclose(fid);
```

APPENDIX D: HISTOLOGY PROTOCOL

After the specimens were extracted the marrow was removed using a water pick. Removing the marrow improved the stain penetration. Prior to mechanical testing, specimens were stained with .02% alizarin complexone for 8 hours to label preexisting micro damage. The specimens were rinsed in deionized water for an hour to remove any unbound alizarin stain. After mechanical testing, the specimens were stained with .05% calcein for eight hours to label micro damage that occurred during mechanical testing. After the second staining, the specimens were rinsed again with deionized water to remove any excess stain.(Nagaraja in-press)

A total of 8 samples were extracted; 4 of the samples were extracted from the horizontal direction and 4 from the vertical direction. A sample from the vertical and horizontal group was used as a control and no testing was performed on these samples. After final staining, specimens were dehydrated in a series of graded alcohols, cleared and embedded in methyl methacrylate(MMA). An Isomet Diamond saw (Buehler Ltd) was used to cut the sample into the 150-200micron thick sections and mounted with Eukitt's mounting medium(EM Sciences, USA) Results were compared to the using visual inspection. The fluorescent microscope (Nikon 5600) was used to find linear and cross-hatched damage. The histology data was matched to the acoustic emission distribution to provide a qualitative analysis.

REFERENCES

Physical Acoustics. (1995). MISTRAS 2001 User's Manual. Princeton, New Jersey, PA Corp.

Alves, J. M. (1996). "Influence of Marrow on Ultrasonic velocity and Attenuation in Bovine Trabecular Bone." Calcified Tissue International **58**: 362-367.

Aue, J. (1998). "A Study of the Mechanical Properties of Highly Porous Ceramics Using Acoustic Emission." Journal of Materials Science **16**: 5455-5462.

Davies, J. (1996). "Monitoring the Integrity of the Cement-Metal Interface of Total Joint Components in vitro Using Acoustic Emission and Ultrasound." Journal of Arthroplasty **Vol.11**(No. 5): 594-601.

Fischer, R. (1986). "Analysis of the Effect of Using Two Different Strain Rates on the Aacoustic Emission in Bone." Journal of biomechanics **19**(2): 119-127.

Ford, C. (1996). "The Dependence of Shear Failure Properties of Trabecular Bone on Apparent Density and Trabecular Orientation." Journal of Biomechanics **29**(10): 1309-1317.

Hasegawa, K. (1993). "Mechanical Properties of Osteopenic Vertebral Bodies Monitored by acoustic Emission." Bone **14**: 737-743.

Hatton, C. G. (1993). "A Comparison of Seismic and Structural Measurement of Scaling Exponents During Tensile Subcritical Crack Growth." Journal of Structural Geology **15**(12): 1485-1495.

Hayes, W. (1997). Biomechanics of Cortical and Trabecular Bone: Implications for Assessment of Fracture Risk. Basic Orthopaedic Biomechanics. H. Mow . Philadelphia, Lippincott-raven.

Keaveny, T. (1994). "Mechanical Behaviour of Damaged Trabecular Bone." Journal of Mechanical bone **27**(11): 1309-1318.

Kohn, D. (1995). "Acoustic Emission and Nondestructive evaluation of Biomaterials and Tissues." Critical reviews in Biomedical Engineering **22**(3): 221-306.

Konstankiewicz, K. (2000). "Method of Acoustic Emission in the Studies of Cracking Processes in Plant Tissues." Electronic Journal of Polish Agricultural Universities **3**(2): 1-12.

Miller, D. (2004). "Membrane Damage Thresholds for 1-10MHz pulsed ultrasound exposure of Phagocytic Cells Loaded with Contrast Agent Gas Bodies in-vitro." Ultrasound Medical Biology **30**(3): 405-111.

Morgan, E. (2001). "Dependence of Yield Strain of Human Trabecular Bone on Anatomic Site." Journal of Biomechanics **34**: 569-577.

Nagaraja, S. (in-press). "Trabecular Damage and Micorstructural Stresses under Uniaxial Compression." Journal of Biomechanics.

Petri, A. (1994). "Experimental Evidence for Critical Daynamics in Microfracturing Processes." Physical Review Letters **73**(25): 3423-3426.

Qi, G. (2000). "3-D AE Visulaization of Bone-Cement Fatigue Locations." Journal of Biomeidcal Material Research **52**: 256-260.

Reasenberg, P. (1989). The Distribution Of Earthquakes--Activity#9. www.data.scec.org/Module/s2act09.html

Reasenberg, P. (1989). "Earthquake Hazard After a Mainshock in California." Science **243**: 1173-1176.

Wear, K. (2000). "Anisotropy of Ultrasonic Backscatter and Attenuation from Human Calcaneus: Implications for Relative Roles of Absorption and scattering in Determining Attenuation." Journal of the Acoustical Society of America **107**(6): 3474-3478.

Wear, K. (2001). "A numerical Method to Predict the Effects of Frequency Dependent Attenuation and Dispersion on Speed of Sound Estimates in Cancellous Bone." Journal of the Acoustical Society of America **109**(3): 1213-1218.

Wolfgang, S. Y., K (1991). Acoustic Emission: Current Practice and Future Directions. Philadelphia, ASTM.